Acta Crystallographica Section B
Structural Science
ISSN 0108-7681

Thermal motion of *tert*-butyl groups III. *tert*-Butyl substituents in aromatic hydrocarbons, the view from the bottom of the well

Joseph Frey,[a] Saeed I. Khan,[b] Carolyn B. Knobler,[b] David A. Lightner,[c] Emily F. Maverick,[b]* Daniel J. Phillips,[d] Zvi Rappoport[e] and Kenneth N. Trueblood[b]‡

[a]Department of Chemistry, Bar Ilan University, Ramat-Gan 52900, Israel, [b]University of California, Los Angeles, CA 90095-1569, USA, [c]University of Nevada, Reno, NV 89557, USA, [d]Bethany College, Bethany, WV 26032, USA, and [e]The Hebrew University, Jerusalem 91904, Israel

‡ Deceased May 1998.

Correspondence e-mail: maverick@chem.ucla.edu

Received 7 April 2010
Accepted 7 October 2010

The rigidity of the *tert*-butyl group (TBG) as a substituent in aromatic hydrocarbons is investigated, with a modified Hirshfeld test of anisotropic displacement parameters (ADPs) as a primary criterion. Four new structures are analyzed, along with low-temperature studies of a previously published crowded supermesityl dimer; three of the five structures meet the primary test. Most of the TBGs meet the Hirshfeld test at 100 K, and the ADPs are improved by omitting low-order data in the final refinement. The three most precise structures yield a wide variation in libration amplitudes (and in estimated rotation barriers) for 13 unique TBGs. A similar range of values is found in analyses of structures in the Cambridge Crystallographic Database. The libration amplitudes are calculated with the program *THMA*14*C*, with each TBG as an attached rigid group (ARG). Packing analysis suggests that large ADPs, *especially for some individual TBG methyl groups*, correspond to voids in the crystal. Published barriers to TBG reorientation, determined by solid-state NMR spin-lattice relaxation methods, for six related crystalline compounds are compared with barriers calculated from their crystal structure data.

1. Introduction

The ADP ellipsoids of *tert*-butyl groups in crystal structures are often elongated, suggesting motion or disorder in the solid state (for Part II, see Maverick *et al.*, 2003). Can a reasonable model for motion be fitted to the ellipsoids? Does the model deduced from the crystal structure lead to agreement with other methods of measuring such motion?

This study presents the analysis of the ADPs of crystal structures of the supermesityl compounds (I) and (II), of the related aromatic hydrocarbons (III) and (IV), and of three new helicenes with TBG substituents, (V) through (VII).[1] Thermal motion analyses employ the program *THMA*14*C* (Farrugia, 1999; Schomaker & Trueblood, 1998). If the TBG can be considered 'rigid' (Hirshfeld, 1976; Rosenfield *et al.*, 1978), a torsional model for its motion is tested and possible barriers to the motion are proposed.

The following primary test (after Hirshfeld) for rigidity is used: the mean e.s.d. (U^{ij}) (*i.e.* the MESDU) for all anisotropic atoms must be ≤ 0.001 Å^2. Low-temperature crystal structures of (II), (III), (V) and (VII) meet this test; they contain a total of 16 unique *ortho*, *meta* and *para* TBGs, in different intramolecular and intermolecular environments.

Thermal motion analysis often suggests that the three methyl C atoms in the TBG are 'moving' with respect to the

[1] Previously published: (I) (Maverick *et al.*, 1991), (II) (Cowley *et al.*, 1997) and (III) at room temperature (Frey *et al.*, 1991). New structures: (III) at 100 and 145 K, (IV), (V), (VI) and (VII).

aromatic core. [For example, the TBGs were excluded from an early thermal motion analysis of di-*tert*-butylpyrene because calculations showed that the entire molecule could not be considered rigid (Hazell & Lomborg, 1972).] In drawings, the ellipsoids of the methyl C atoms often seem consistent with a torsional motion of the group about the $C_{Ar}-C_t$ bond. Ellipsoids for three TBGs [from structures (V), (VII) and (II)] are shown in Fig. 1.

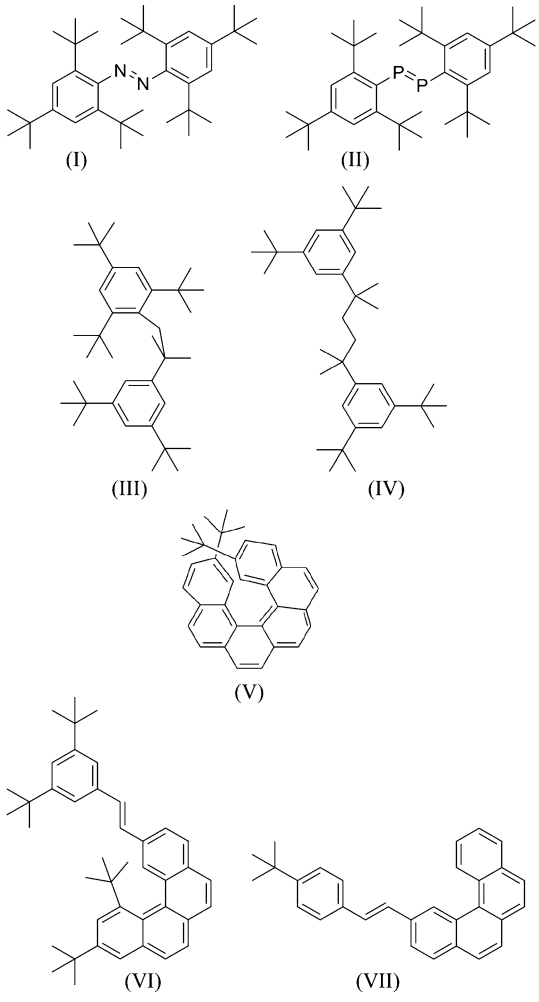

Solid-state barriers to the reorientation of several TBGs attached to aromatic rings have recently been determined by NMR relaxation studies (Beckmann *et al.*, 2009; Rheingold *et al.*, 2008). The torsional motion modelled by ADP analysis, like the NMR model, should reflect intramolecular variations as well as the influence of packing in the crystal.

2. Background

In two previous publications we utilized the atomic displacement parameters (ADPs) determined by conventional crystal structure determinations to predict the barriers to rotational motion of TBGs. The more recent study (Maverick *et al.*, 2003) involved *tert*-butyl ammonium ions complexed to modified crown-ether hosts. Three TBG methyl H atoms form C—H···O contacts with these hosts, suggesting a threefold rotation model.

An earlier study (Maverick *et al.*, 1991) of 2,2′,4,4′,6,6′-hexa-*tert*-butylazobenzene (I) employed two crystals over a wide range of temperatures. Indications of disorder were observed even at low temperatures, and it was not clear whether sixfold or threefold rotation models were more suitable. Differences in calculated barriers for chemically equivalent TBGs indicated the importance of packing, and attempts were made to model changes in inter- and intramolecular energies under TBG rotation. Force-field calculations suggested sixfold rotations with unequal well depths for the 4, 4′ (*para*) TBGs.

In both of these studies the lack of *precision* of the ADPs was noted. Hirshfeld's 'rigid-bond' test (Hirshfeld, 1976) was not satisfied. The Hirshfeld test utilizes the differences in mean-square displacement amplitudes (ΔMSDA, calculated from the ADPs) along bonding directions. The ADPs are considered to be adequate to distinguish vibration from bond deformation or disorder if the ΔMSDA along each bonding direction in the molecule is 'well under 0.001 $Å^2$'. In this work a modified Hirshfeld test is used to select and judge TBGs for rigidity as ARGs.

Hirshfeld recommended that high-order data and a multipole or deformation-density refinement procedure be used to obtain ADPs of high quality. Multipole refinement with high-angle [$\sin(\Theta)/\lambda = 0.90$] data was used in the electron-density distribution study of the diphosphene (II) at 100 K (Cowley *et al.*, 1997). The resulting ADPs satisfy the 'rigid-bond' test quite well. The structure of (II) serves as a model for ADP analysis (see §4.2).

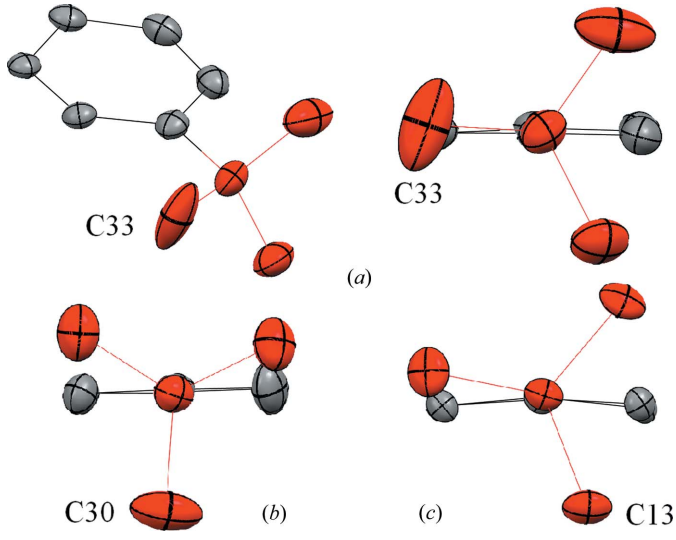

Figure 1
Views of three TBG groups with attached six-membered aromatic ring; ring *C* atoms in black, TBG C atoms in red. All ellipsoids enclose 50% probability (CSD *Mercury*; Macrae *et al.*, 2008). (*a*) Two views of ring atoms C13–C18 and TBG atoms C31–C34, structure (V*a*). Left, a perspective view. Right, these 10 atoms viewed down the C_t-C_{Ar} bond. C33 is labelled. See Fig. 5. C33 almost eclipses a ring carbon (C16). (*b*) Atoms C1–C4, C25–C30, structure (VII*a*). View down the C_t-C_{Ar} bond; see Fig. 7. None of the methyl C atoms eclipses a ring atom. (*c*) A similar view of the *para* TBG in structure (II) (Cowley *et al.*, 1997); see Fig. 8.

The separation of thermal and bonding effects in ADPs in crystal structure determinations continues to be of interest. For example, studies of hydrochlorides of L-hydroxylysine (Dittrich *et al.*, 2008) employed invariom and multipole refinement on F with data to $\sin(\Theta)/\lambda = 0.90$ or greater, and demonstrated improvement in the ADPs (by the Hirshfeld test) by omitting reflections with $\sin(\Theta)/\lambda < 0.4$. Bendeif *et al.* (2009) used standard refinement on F^2, with data collected to $\sin(\Theta)/\lambda = 0.7$ at multiple temperatures, to analyze changes in ADPs related to a phase transition. McMullan *et al.* (2008) used neutron data to study thermal motion in three phases of deuterated γ-malonic acid. ADP analysis suggested large librational motion even at 50 K; the refinement of the ADPs was modified to include anharmonic terms. Bürgi *et al.* (2000) developed a quasi-harmonic method for separating the contributions to the ADPs into temperature-dependent and temperature-independent parts (such as internal vibrations and absorption or extinction errors).

The current checking procedure for CIFs by the IUCr applies the ΔMSDA check, and notes large deviations from the above standard. The CIF dictionary (entry **PLAT234** Type_4) refers to possible contamination of the ADPs by substitutional disorder, model errors, absorption correction errors or overrefinement.

TBGs as substituents in aromatic rings have many uses. Solution ^{1}H NMR studies and molecular mechanics calculations indicated that rotational barriers were usually low, and might range from ~ 2 to ~ 40 kJ mol^{-1} (Anderson *et al.*, 1972; Yamamoto & Ōki, 1986). Such adaptability may contribute to the useful properties of the *p-tert*-butylphenyl group. For example, *p-tert*-butylphenol has been a precursor of choice to provide good yields in a 'one-step' calixarene synthesis (Gutsche & Lin, 1986), and the *p-tert*-butylphenyl group as a substituent promotes the self-assembly of one-dimensional fullerene stacks (Kennedy *et al.*, 2008). 'Crowding' owing to neighbouring TBG substituents can produce the loss of aromaticity observable by crystallographic, spectroscopic and molecular mechanics methods (Sakai, 1978; Handal *et al.*, 1977). Compound (II), 'the first isolated compound with a phosphorus-phosphorus double bond', is stabilized by steric hindrance owing to the TBG substituents (Yoshifuji *et al.*, 1981). Three TBGs stabilize (or make 'persistent') the 2,4,6-tri-*tert*-butylphenyl (supermesityl) radical to aid in dimer formation, producing compounds (III) and (IV) (Frey *et al.*, 1991; Johnson & Hawthorne, 1991). In the synthesis of 2,15-di-*tert*-butylhexahelicene [(V), this work], two TBGs were introduced with the goal of expanding the gap between the terminal rings (Phillips, 2002).

2.1. Models for torsional motion

Seeman *et al.* (1989) determined by low-temperature jet laser spectroscopy that in the lowest-energy conformation for gas-phase aromatic TBGs one of the methyls lies in the aromatic plane (termed a 'planar' conformation). The 'perpendicular' and the '*gauche*' conformations, representing 30 and 15° rotations about the $C_{Ar}-C_t$ bond from the planar minimum were also considered. All three conformations are found in crystal structures. The examples in Fig. 1 show that (*a*) is a nearly 'planar', (*b*) is a nearly 'perpendicular' and (*c*) is a nearly '*gauche*' conformation.

The model for solid-state rigid-group torsional motion may propose either a threefold or a sixfold rotation. If the conformation is 'planar', and there are other substituents on the aromatic ring, a threefold rotation may be required to achieve a chemically equivalent position. If the conformation is 'perpendicular' or '*gauche*', then a sixfold rotation may produce a chemically equivalent structure. Reorientation would be necessary since in a typical TBG substituent the $C_{Ar}-C_t-C_{Me}$ angles differ, from ~ 108 to 112°, and the C_t-C_{Me} distances are not equal (see §4.6 for examples from this work).

Whereas the threefold rotation should produce the same *intermolecular* interactions if angles and distances readjust, the sixfold rotation might not. Barriers estimated at 100 K for the *para* TBGs in molecule (I) were ~ 7 kJ mol^{-1} for a sixfold and ~ 23–25 kJ mol^{-1} for a threefold rotation. The twofold disorder model employed for molecule (I) at higher temperatures [and for molecules (III*a*) and (VI) below] suggests sixfold TBG reorientation; if the occupancies at the two minima differ, two different well depths are implied (Maverick *et al.*, 1991). The difficulties associated with employing ADPs to analyze motion of TBGs in the solid state are:

(i) barrier height is deduced from libration amplitudes, calculated 'at the bottom of the well', with a very different well width for sixfold and threefold rotations;

(ii) there is no simple way to incorporate individual methyl reorientation or the lack of threefold symmetry in the model;

(iii) the nine H atoms, whose positions are important in intra- and intermolecular contacts, are not well located in X-ray structures.

In addition, it is not possible to separate the libration of the *ARG* from the overall libration of the *molecule* parallel to the ARG axis[2] (Schomaker & Trueblood, 1998).

2.2. Energy barriers to reorientation

Beckmann and co-workers (Beckmann, 1981; Beckmann *et al.*, 1988, 1994, 2009; Rheingold *et al.*, 2008) have determined activation energies for the reorientation of TBGs (as substituents in aromatic compounds) in crystals by nuclear spin-lattice relaxation. Energy values for barriers range from 16 to 32 kJ mol^{-1} for motions described as 'hops' (rather than harmonic or torsional reorientations). Two types of 'planar' conformations have been proposed. In the 'planar' Type *A* model the three methyls are dynamically equivalent, and they reorient along with the TBG, perhaps by a gearing process. Type *A* is expected if both substituents *ortho* to the TBG are H atoms; the TBGs reorient in sixfold potential wells. In 'planar'

[2] In the terms used in *THMA*14*C*, $\langle\Phi^2\rangle$ (calculated in the program) is equal to the libration amplitude of the ARG, (φ^2), $+2(\varphi\lambda^{\parallel})$. It is approximately equal to (φ^2) only if the parallel overall motion of the molecule, $\lambda^{\parallel}$, is small compared with φ.

Table 1
Experimental details for low-temperature structures with Mo $K\alpha$ radiation.

H-atom parameters were constrained; results of high-order refinements for (III*a*), (V*a*) and (VII*a*) are included.

	(III*a*)	(III*b*)	(IV*a*)	(V*a*)
Crystal data				
Chemical formula	$C_{36}H_{58}$	$C_{36}H_{58}$	$C_{36}H_{58}$	$C_{34}H_{31.98}I_{0.02}$
M_r	490.82	490.82	490.82	443.11
Crystal system, space group	Triclinic, $P\overline{1}$	Triclinic, $P\overline{1}$	Triclinic, $P\overline{1}$	Orthorhombic, *Pbca*
Temperature (K)	100	145	128	100
a, b, c (Å)	15.7799 (17), 19.394 (2), 10.5789 (11)	15.850 (4), 19.464 (5), 10.596 (3)	9.8680 (7), 9.9061 (7), 9.9285 (7)	9.7668 (8), 16.5318 (14), 30.463 (3)
α, β, γ (°)	94.982 (1), 95.188 (1), 89.963 (2)	95.112 (11), 95.102 (11), 90.084 (9)	77.626 (3), 60.758 (3), 76.286 (3)	90, 90, 90
V (Å^3)	3212.1 (6)	3243.0 (15)	817.15 (10)	4918.7 (7)
Z	4	4	1	8
μ (mm^{-1})	0.06	0.06	0.06	0.09
Crystal size (mm)	0.40 × 0.36 × 0.16	0.60 × 0.34 × 0.23	0.45 × 0.4 × 0.2	0.58 × 0.15 × 0.15
Data collection				
Diffractometer	CCD area detector	Modified Picker FACS1	Modified Picker FACS1	CCD area detector
Absorption correction	Multi-scan *SADABS* (Bruker)	–	–	Multi-scan *SADABS* (Bruker)
T_{min}, T_{max}	0.898, 0.991	–	–	0.776, 0.99
No. of measured, independent and observed $[I > 2\sigma(I)]$ reflections	42 208, 16 793, 11 868 (full data) 21 193, 10 124, 6146 (high)	8738, 8593, 4272	4751, 4751, 2086	30 137, 6020, 4289 (full data) 19 817, 4540, 2945 (high)
R_{int}	0.037 (full), 0.104 (high)	0.0000	0.0000	0.036 (full), 0.082 (high)
Refinement				
$R[F^2 > 2\sigma(F^2)]$, $wR(F^2)$, S	0.047, 0.129, 1.02 (full) 0.053, 0.138, 0.99 (high)	0.086, 0.258, 1.08	0.077, 0.228, 1.06	0.046, 0.127, 1.03 (full) 0.049, 0.131, 1.04 (high)
No. of reflections	16 793 (full) 10 124 (high)	8593	4751	6020 (full) 4540 (high)
No. of parameters	696, 693 (high)	652	171	331
No. of restraints	6	18	0	0
$\Delta\rho_{max}$, $\Delta\rho_{min}$ (e Å^{-3})	0.38, −0.21 (full) 0.15, −0.13 (high)	0.35, −0.38	0.39, −0.42	0.30, −0.21 (full) 0.19, −0.17 (high)

	(VI)	(VII*a*)	(I)
Crystal data			
Chemical formula	$C_{42}H_{50}$	$C_{30}H_{26}$	$C_{36}H_{58}N_2$
M_r	554.82	386.51	518.84
Crystal system, space group	Monoclinic, $P2_1$	Monoclinic, $P2_1/c$	Orthorhombic, *Pbca*
Temperature (K)	100	100	100
a, b, c (Å)	9.7954 (7), 28.071 (2), 12.5190 (9)	15.8912 (15), 15.3430 (14), 8.6285 (8)	16.495 (3), 17.360 (3), 23.009 (4)
α, β, γ (°)	90, 96.349 (1), 90	90, 92.680 (2), 90	90, 90, 90
V (Å^3)	3421.2 (4)	2101.5 (3)	6588.7 (18)
Z	4	4	8
μ (mm^{-1})	0.06	0.07	0.06
Crystal size (mm)	0.3 × 0.2 × 0.1	0.6 × 0.18 × 0.10	0.50 × 0.50 × 0.30
Data collection			
Diffractometer	CCD area detector	CCD area detector	Modified Huber
Absorption correction	Multi-scan *SADABS* (Bruker)	Multi-scan *SADABS* (Bruker)	–
T_{min}, T_{max}	0.511, 1.0	0.630, 0.993	–
No. of measured, independent and observed $[I > 2\sigma(I)]$ reflections	22 479, 8320, 4267	13 315, 5024, 3123 (full data) 8635, 3750, 2057 (high)	10 284, 5809, 3646
R_{int}	0.066	0.036 (full), 0.081 (high)	0.087
Refinement			
$R[F^2 > 2\sigma(F^2)]$, $wR(F^2)$, S	0.066, 0.186, 1.00	0.048, 0.136, 1.02 (full data) 0.057, 0.160, 1.02 (high)	0.085, 0.240, 1.07
No. of reflections	8320	5024, 3750 (high)	5809
No. of parameters	761	274, 181 (high)	361
No. of restraints	49	0	0
$\Delta\rho_{max}$, $\Delta\rho_{min}$ (e Å^{-3})	0.49, −0.32	0.27, −0.24 (full) 0.19, −0.18 (high)	0.26, −0.34

Computer programs used: *SMART APEX*2 (Bruker, 2007), UCLA (1984), *SAINT* (Bruker, 2007), *SHELXS*97, *SHELXL*97 (Sheldrick, 2008), *SADABS* (Bruker, 2007).

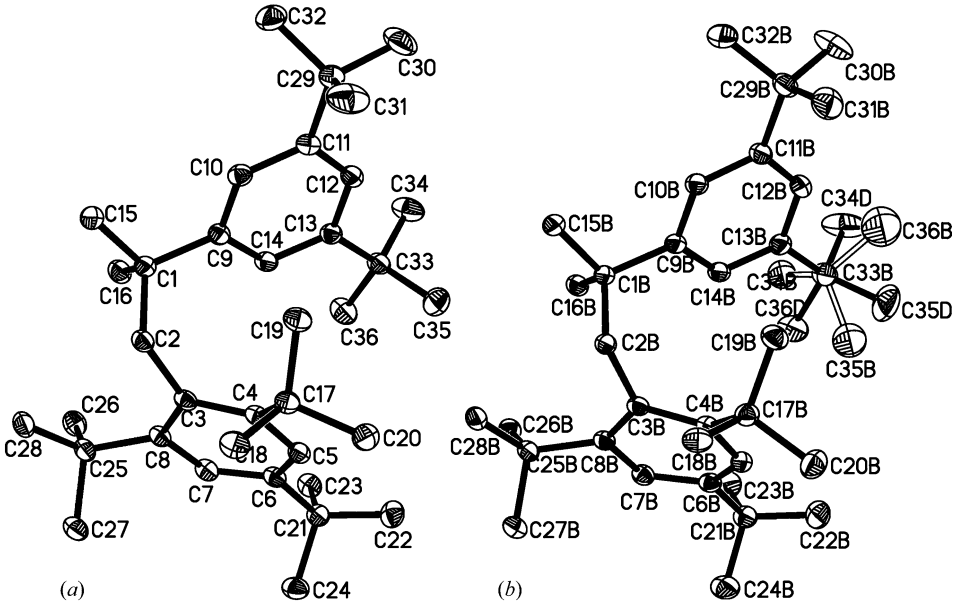

Figure 2
Structure of (III*a*), with atomic numbering: two molecules in the asymmetric unit. (*a*) Molecule (1); (*b*) molecule (2) (labelled C1*B etc.*). H atoms omitted for clarity. Ellipsoids enclose 50% probability. The views are chosen to show the five independent TBGs in each molecule and the close approach of C19 (C19*B*) to the C9–C14 (C9*B*–C14*B*) rings.

Type *B* two methyls are intramolecularly equivalent and the third is different. Type *B* is expected if an *ortho* substituent is other than H (—OH or —Br, for example); the reorientation is a threefold process (Beckmann *et al.*, 1988; Beckmann, 1989; Fry *et al.*, 1991). In recent examples, however, some 'planar' Type *A* TBG models have been found to include two distinct methyl reorientation rates (Beckmann *et al.*, 2004, 2009).

Beckmann's classification has been adopted in this work, as follows: Type *A* and Type *B* groups assume a methyl group eclipsing a ring carbon, as in Fig. 1(*a*). Type *B* has a non-hydrogen *ortho* substituent at the ring carbon opposite the planar TBG methyl group (there are no Type *B* TBGs in Fig. 1). To cover the geometry observed here and in the literature, another class is needed. We use the label 'Type *C*' for conformations like that in Fig. 1(*b*), a 'perpendicular' conformation. In some structures, the tertiary carbon is bent out of the aromatic plane, or the ring itself is non-planar, as in Fig. 1(*c*). Such TBGs are also designated *C*, or if the conformation is nearly 'planar', *A*–*C* or *B*–*C*.

3. Experimental

The preparation of (III) and (IV) has been reported (Frey *et al.*, 1991); syntheses of (V), (VI) and (VII) (Phillips, 2002) are summarized in the supplementary material.[3]

Crystal structures at 100–145 K have been determined for these five compounds (Table 1). Data for high-order refinements of (III*a*), (V*a*) and (VII*a*) are also given. Compound (I) (Maverick *et al.*, 1991) at 100 K has been re-refined, using all reflections. Whereas the earlier refinement had included only reflections with $F > 3\sigma(F)$ (negative intensities had been discarded), the present refinement includes low and negative (as zero) intensities. The increased number of unique reflections (5809 *versus* 4091) and refinement on F^2 result in a better goodness-of-fit. The treatment of H atoms has been altered to correspond with that in compounds (III)–(VII).

In addition, structures for compounds (IV), (V) and (VII) have been determined at room temperature and/or with Cu $K\alpha$ radiation. Table 1A with experimental details is included in the supplementary material.

For ADP analysis of these structures, the following definitions and abbreviations are used:

(i) Mean e.s.d. $(U^{ij}) = \langle \text{e.s.d.}\ (U^{ij})^2 \rangle^{1/2} = (\text{MESDU})$;

(ii) primary MESDU test (after Hirshfeld) = MESDU for all anisotropic atoms ≤ 0.001 Å^2;

(iii) mean $\Delta\text{MSDA} = \langle \Delta\text{MSDA}^2 \rangle^{1/2} = (\text{RMS}\Delta)$;

(iv) Hirshfeld 'rigid-bond' test: ΔMSDA along each bonding direction ≤ 0.001 Å^2;

(v) modified rigid-bond test = (RMSΔ(bonding))/(MESDU) ≤ 3.0;

(vi) TBG rigidity test = TBGR = (RMSΔ(intra-group methyl–methyl))/(MESDU) ≤ 3.0.

If the TBG is moving as a rigid group, the three methyl C atoms should obey the Hirshfeld test: their mean ΔMSDA *along interatomic directions* should be less than 0.001 Å^2. [The TBGR test applied here is less strict, since the mean e.s.d. (U^{ij}) for TBG methyl C atoms is usually larger than the overall MESDU.] Table 2 gives the MESDU and TBGR tests, with the resolution of the data and Z' for all structures.

3.1. Compound (III)

The analysis of the crystal structure of 1-(2,4,6-tri-*tert*-butylphenyl)-2-(3,5-di-*tert*-butylphenyl)-2-methylpropane (III) was originally performed at room temperature (Frey *et al.*, 1991). In 1991 the structure was redetermined at 145 K, in the same unit cell and with the same atomic numbering as for the room-temperature structure. New data on the same crystal have recently been taken at 100 K. The crystal is smaller after 18 years in storage, but more data are collected at 100 K; the 100 K structure is labelled (III*a*) and the 145 K structure (III*b*) in Table 1. Each of the two molecules in the asymmetric

[3] Supplementary data for this paper are available from the IUCr electronic archives (Reference: BK5096). Services for accessing these data are described at the back of the journal.

Table 2
Rigidity tests for *tert*-butyl groups in the structures in Table 1 and Table 1A (supplementary material).

See text for MESDU and TBGR definitions.

Structure	T (K)	Z'	Radiation	Θ^{max}	MESDU	TBGR
(III*a*)	100	2	Mo $K\alpha$	29.17	0.0006	0.3–2.5†
(III*a*) high	100	2	Mo $K\alpha$	29.17	0.0007	0.4–2.5†
(III*b*)	145	2	Mo $K\alpha$	27.0	0.0033	1.2–3.9†
(IV*a*)	128	0.5	Mo $K\alpha$	30.0	0.0014	2.2, 2.4
(V*a*)	100	1	Mo $K\alpha$	28.31	0.0007	1.3, 8.8
(V*a*) high	100	1	Mo $K\alpha$	28.31	0.0007	1.3, 8.2
(VI)	100	2	Mo $K\alpha$	28.31	0.0032	0.8–2.8†
(VII*a*)	100	1	Mo $K\alpha$	28.27	0.0008	2.5
(VII*a*) high	100	1	Mo $K\alpha$	28.27	0.0010	2.5
(I) (re-refined)	100	1	Mo $K\alpha$	25.0	0.0017	0.9–2.4
(IV*b*)	293	0.5	Mo $K\alpha$	30.0	0.0017	4.0, 4.5
(V*b*)	100	1	Cu $K\alpha$	67.75	0.0007	0.7, 9.2
(V*c*)	298	1	Mo $K\alpha$	28.29	0.0013	1.3, 12.5
(V*d*)	298	1	Cu $K\alpha$	64.47	0.0014	2.3†
(VII*b*)	100	1	Cu $K\alpha$	68.12	0.0006	3.9
(VII*c*)	298	1	Mo $K\alpha$	28.34	0.0014	6.7
(VII*d*)	298	1	Cu $K\alpha$	64.68	0.0012	7.6

† One or more TBGs omitted or treated as disordered.

unit contains five crystallographically unique TBGs: two *ortho*, two *meta* and one *para* to the bridging dimethylethyl group (Fig. 2).

Structure (III*a*) meets the MESDU test while (III*b*) does not (Table 2); one TBG has been refined with a disorder model in each structure, a twofold model [0.920 (3)/0.080 (3) occupancy ratio] at 100 K and a threefold model (occupancies 0.46/0.39/0.15, held constant in the final refinement) at 145 K. Structure (III*b*) was originally refined on F, negative intensities were discarded and duplicates merged; the present refinement on F^2 uses the incomplete data set (no zero or negative intensities).

Distances are poor in the disordered region (C_t-C_{Me} 1.48–1.59 Å at 145 K and 1.49–1.61 Å at 100 K), although restraints were employed. ADPs were refined for C34*D*—C36*D*, the major conformer in (III*a*) (Fig. 2). The disorder model consists of two Type *A* TBGs, with C36*D* and C36*B* approximately eclipsing the ring; C36*B* and C34*D* are 0.99 Å apart, and have the largest U_{equiv} values; the ellipsoid for C34*D* is highly oblate (Fig. 2).

The two independent molecules are twisted so that the TBGs C17–C20 and C17*B*–C20*B* face the planes of rings C9–C14 and C9*B*–C14*B*. The geometry suggests intramolecular C—H$\cdots\pi$ contacts (Desiraju, 2002). The tetra-substituted, or supermesityl, rings show large deviations from typical aromatic distances and angles, as the room-temperature study suggested (Frey *et al.*, 1991). Selected angles and distances are recorded in Table 3A in the supplementary material. The aromaticity of these rings is further disturbed by the displacement of C2 and C2*B*, and the *ortho* tertiary C atoms C17, C25, C17*B* and C25*B* from the attached ring planes (from 0.44 to 0. 60 Å). The *ortho* TBGs are displaced away from the centre of each molecule (Fig. 3). The *para* C atoms in (III*a*), C21 (−0.06 Å) and C21*B* (0.16 Å) lie closer to their respective ring planes. [These distortions of the supermesityl rings are greater than those in (I) and (II); for example, the *ortho* tertiary C atoms are displaced from the attached ring planes by 0.23–0.38 Å in (I), and 0.16–0.36 Å in (II).]

The trisubstituted ring retains more typical aromatic distances and angles, and the *meta* C atoms C29, C33 (and C29*B*, C33*B*) lie more closely within their respective ring

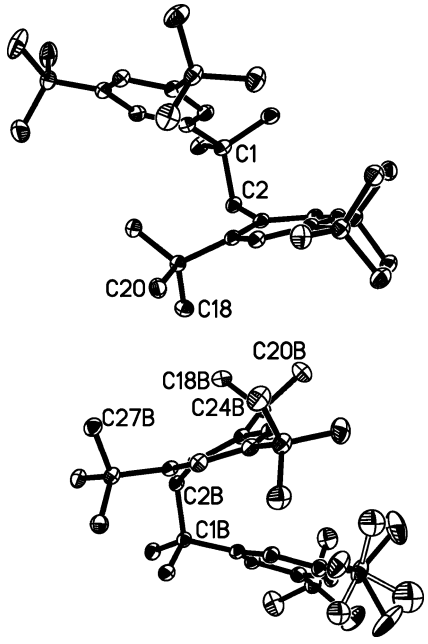

Figure 3
The two independent molecules in the asymmetric unit of structure (III*a*), showing the close approach of TBG C17–C20 to the tetra-substituted ring of the *B* molecule. The cell axis *a* is approximately vertical in this view (x = 0, top, x = 1, bottom); most labels and all the H atoms have been omitted.

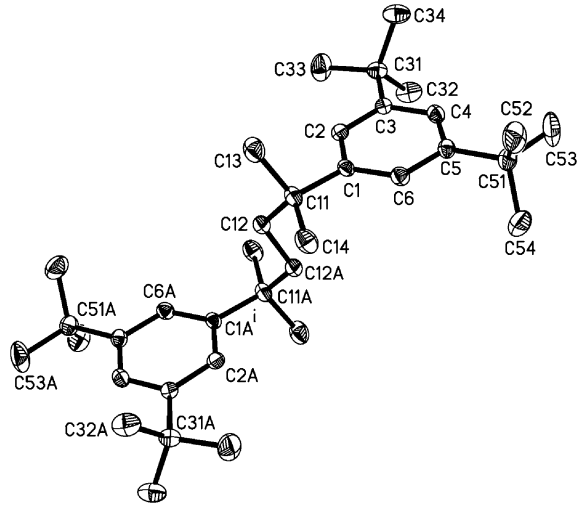

Figure 4
Structure of (IV*a*), showing atomic numbering. H atoms omitted. Symmetry code: (i) $-x+1, -y+1, -z+2$ (centre between C12 and C12*A*); some labels for the *A* atoms have been omitted. Ellipsoids enclose 50% probability.

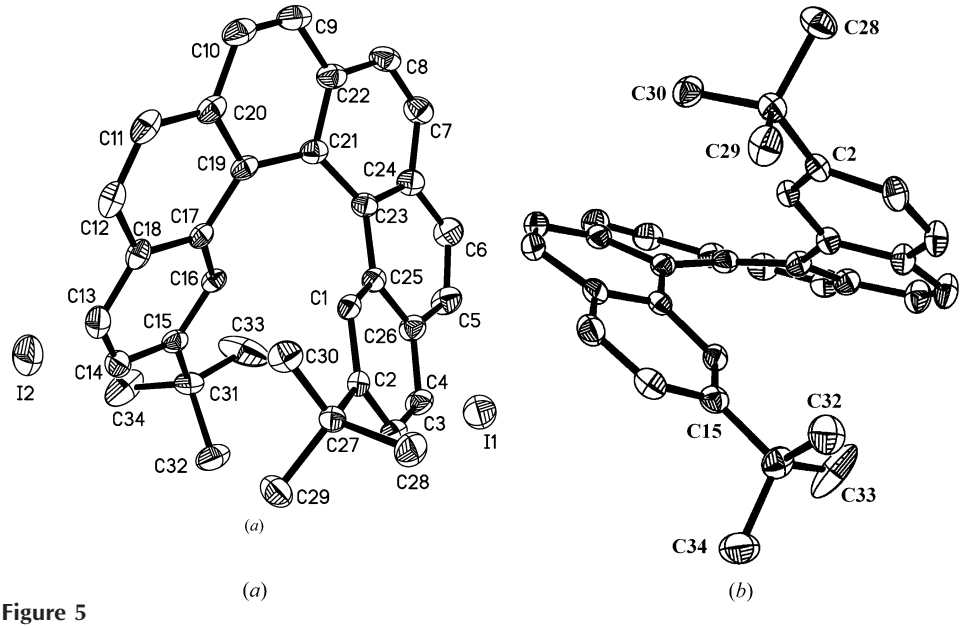

Figure 5
Structure of (V*a*), 2,15-di-*tert*-butylhexahelicene. (*a*) Atomic numbering; (*b*) perspective view showing the orientation of the TBGs in relation to the hexahelicene moiety. H atoms omitted. Atoms I1 and I2 refined with occupancies of 0.01 each (see text); iodine atoms omitted in (*b*). Ellipsoids enclose 50% probability.

planes (less than 0.04 Å). The *ortho* TBGs are labelled Type *C*, and the *meta* and *para* TBGs are designated Type *C* or *A*–*C* (§2.2).

3.2. Compound (IV)

2,5-Bis(3,5-di-*tert*-butylphenyl)-2,5-dimethylhexane (IV) is a structural isomer of compound (III). It is the 2–2 dimer of the 2,4,6-tri-*tert*-butylphenyl radical, whereas (III) is the 1–2 dimer (Frey *et al.*, 1991). The data for (IV*a*) were collected at 128 K, and originally refined on *F*. Negative intensities were discarded and duplicates were merged. Recent refinement on F^2 uses an incomplete data set, with zero *and* negative intensities set to 0.00. The MESDU test is not met (Table 2). The molecule lies on a centre of symmetry; the two *meta* TBGs in the asymmetric unit are chemically equivalent (Fig. 4). The tertiary C atoms are approximately coplanar with the aromatic ring (0.006 and 0.009 Å, r.m.s. deviation of the plane 0.003 Å). The TBGs are Type *A*; the conformation resembles two linked molecules of 1,3,5-tri-*tert*-butylbenzene. The structure of the latter is disordered at room temperature (Sakai, 1978).

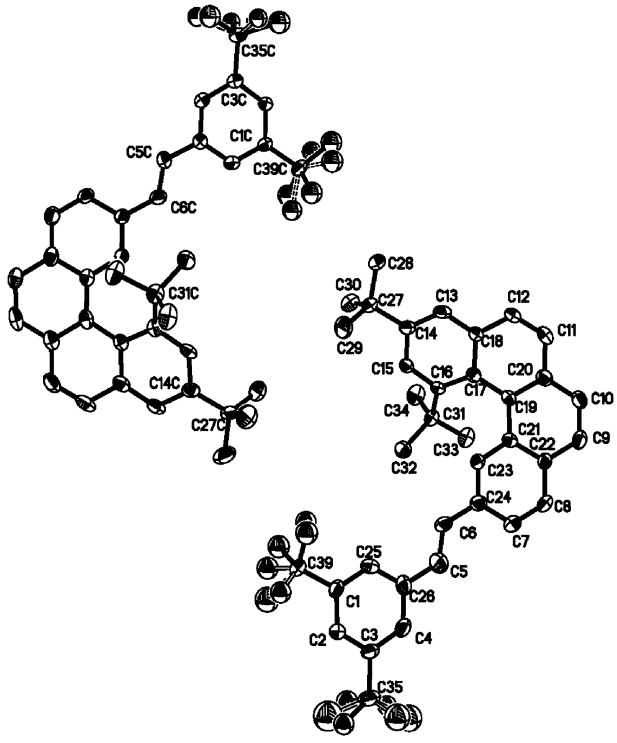

Figure 6
Structure of (VI); the view is chosen to show the atom numbering, which corresponds to that of the desired hexahelicene product. H atoms, labels for disordered *tert*-butyl groups, and most labels for the second molecule in the asymmetric unit are omitted. Ellipsoids enclose 50% probability.

3.3. Compound (V)

(±)-2,15-Di-*tert*-butylhexahelicene (Fig. 5) crystallizes in the space group *Pbca* with $Z = 8$. Atomic numbering corresponds to that used in earlier hexahelicene structures (Frank *et al.*, 1973). The distances from two small residual peaks (after refinement of the $C_{34}H_{32}$ moiety) to nearby C atoms suggested iodine; since iodine had been present in the synthesis [Phillips, 2002; see supplementary material for a summary of the syntheses of (V), (VI) and (VII)] the peaks were refined as iodine atoms. The final occupancy of each iodine was 0.01 and that of each of the two H atoms (H4 and H13, bound to the respective C4 and C13 atoms near I1 and I2) was 0.99. Our model thus assumes the presence of a very small amount of iodinated impurity in the crystals. In spite of the apparent impurity, the refined distances and angles are consistent with those in other hexahelicenes (Frank *et al.*, 1973; Behm *et al.*, 1988), and the MESDU criterion is met (Table 2).

The C2···C15 distance, a measure of the 'gap' between terminal rings, is 4.19 Å, larger than that in 1,16-dimethylhexahelicene (4.03 Å; van den Hark & Noordik, 1973) and in 1,3-di-*tert*-butylhexahelicene (3.95 Å; Behm *et al.*, 1988), but shorter than that in 2-methylhexahelicene (4.45 Å; Frank *et al.*, 1973). In unsubstituted hexahelicene this distance is 4.58 Å in the pure compound (de Rango *et al.*, 1973) and 3.93–4.55 Å in hexahelicene complexes with π-acceptors (Ermer & Neudörfl, 2001). Bond distances differ from those in planar aromatic compounds, as has been noted previously; selected

Table 3
Matrix of differences of observed ΔMSDA for (II) (Cowley *et al.*, 1997), generated by *THMA*14*C*.

Values listed are $10^4 \times$ ΔMSDA (Å^2) for column atom minus that for row atom, along the line between them. MESDU = 0.0010 Å^2; RMSΔ for all atoms = 0.0038 Å^2, RMSΔ for bonded atoms = 0.0016 Å^2. ΔMSDA for bonded atoms underlined; six large non-bonded values in bold type. Rigid group (three TBGs, one phenyl ring) values in italics. 'Position 1' indicates that the model includes one half-molecule only (position 2 is generated by the twofold axis, see Fig. 8*a*).

Atom	C18	C17	C16	C15	C14	C13	C12	C11	C10	C9	C8	C7	C6	C5	C4	C3	C2	C1
Position	1	1	1	1	1	1	1	1	1	1	1	1	1	1	1	1	1	1
P1	11	12	−9	−7	26	38	**40**	23	28	19	31	12	17	18	21	24	38	9
C1	−13	−15	0	−35	15	30	26	13	−21	−31	−27	−25	*−20*	*−12*	*11*	*2*	*−4*	
C2	19	15	10	−7	12	38	5	−6	13	21	−10	17	*6*	*−22*	*9*	*0*		
C3	**40**	17	32	6	1	30	7	−22	1	11	−23	−8	*16*	*−19*	*5*			
C4	30	18	30	−2	9	26	11	2	3	10	−32	−3	*8*	*0*				
C5	16	7	−1	−21	−1	−10	−10	−21	29	23	15	**41**	*−11*					
C6	31	2	13	−11	11	14	2	−4	9	−13	−10	6						
C7	13	−4	5	−15	11	**43**	18	−13	*20*	*6*	*22*							
C8	29	6	8	−4	**41**	**75**	23	−2	*13*	*−6*								
C9	18	14	3	0	−1	20	−17	−35	*6*									
C10	6	−3	−10	−19	1	35	−7	−22										
C11	36	26	25	−2	*29*	*33*	*17*											
C12	23	14	19	−9	*19*	*23*												
C13	−3	−26	7	−34	*−2*													
C14	8	−22	−6	−28														
C15	*24*	*19*	*12*															
C16	*−11*	*16*																
C17	*0*																	

distances, angles and planes for (V*a*) are given in Table 5A in the supplementary material.

The two TBGs are not alike, although both are Type *A* (Fig. 1*a* and §2.2). The ADPs for the C27–C30 group are smaller than those for C31–C34 (U_{equiv} 0.0214–0.0323 *versus* 0.0273–0.0622; see also Fig. 5). The ADPs will be discussed further in §4.

3.4. Compound (VI)

trans-1-(3,5-Di-*tert*-butylphenyl)-2-(3,4-benzo-5,7-di-*tert*-butylphenanthrenyl)ethylene (VI), a tetrahelicene, is the *trans* isomer of an intermediate in the synthesis of 1,3,14,16-tetra-*tert*-butylhexahelicene (Phillips, 2002; see the summary of the synthesis in the supplementary material). There are two molecules in the asymmetric unit. They have opposite chirality (*i.e.* the torsion angles C16—C17—C19—C21 and C16*C*—C17*C*—C19*C*—C21*C* are −31.7 and 33.9°), but no additional crystallographic symmetry could be found (*PLATON*; Spek, 2003). The centroid of the pair in Fig. 6 is at 0.368, 0.404, 0.370 (CSD *Mercury*). The MESDU test is not met (Table 2). The TBGs attached to phenyl rings are disordered, while those attached to the terminal ring of the tetrahelicene moiety are ordered (Fig. 6). The *ortho* tertiary C atoms C31 and C31*C* are displaced ∼ 0.7 Å from the mean planes of the attached six-membered rings (r.m.s. deviation of six fitted atoms about 0.07 Å). Thus, the *ortho* TBGs at C31 and C31*C*, which would be Type *B* if the TBG conformation were 'planar' (see Fig. 1 and §2.2), are classified as Type *C*. The *meta* tertiary C atoms C27 and C27*C* are displaced only ∼ 0.1 Å from the ring planes; these *meta* TBGs are 'planar', Type *A*.

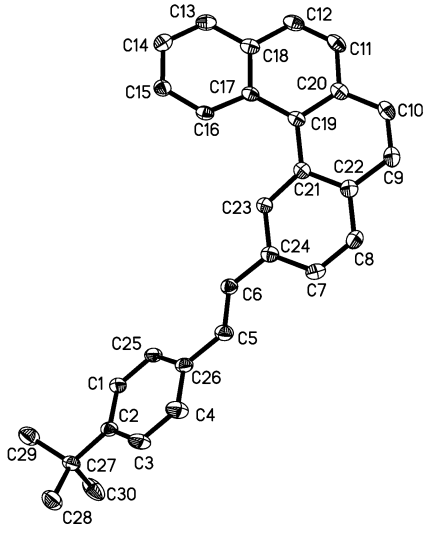

Figure 7
Structure (VII*a*), with atomic numbering. H atoms omitted. Ellipsoids enclose 50% probability.

3.5. Compound (VII)

trans-1-(*para-tert*-Butylphenyl)-2-(2-benzo[c]phenanthrenyl)-ethylene (VII) is also a tetrahelicene. The MESDU criterion is met for structures (VII*a*) and (VII*b*) (Table 2). As shown in Fig. 1, none of the three methyl C atoms eclipses a ring C atom, and the TBG is classified as Type *C* (§2.2). Fig. 7 gives atom numbering, chosen to correspond to that of (V) and (VI). The ellipsoids at C1, C3, C4 and C25 suggest rotational motion of the *p-tert*-butylphenyl moiety about the C26—C2—C27 axis (see §4.2.2).

3.6. Additional crystal structures

Crystal data for additional structural studies of compounds (IV), (V) and (VII) are given in Table 1A in the supplemen-

tary material. Cu $K\alpha$ radiation gave improved agreement factors, $R[F^2 > 2\sigma(F^2)]$, $wR(F^2)$, but not, in general, improved Hirshfeld criteria (Table 2), perhaps owing to the smaller numbers of unique reflections and more limited resolution. Room-temperature structures resulted in higher agreement factors and higher MESDU values. In short, for (III)–(VII), only (III*a*), (V*a*), (V*b*), (VII*a*) and (VII*b*) result in MESDU $\leq$ 0.001 Å^2 – all done at 100 K. None of the higher-temperature structures [nor the disordered (VI)] satisfy this test.

Data for (IV) were collected in 1991. Duplicates were merged and zero and negative intensities were given $F = 0.00$ and arbitrary $\sigma(F)$; with the refinement on $F \geq 3\sigma(F)$, customary at the time, zero-intensity reflections were eliminated. There are 1176 (and 814) $F^2 = 0.00$, out of 4751 (and 4925) unique reflections in (IV*a*) and (IV*b*). The present refinements with 'all data' are strongly affected by the choice of $\sigma(F^2)$ for these unknown (but very low or negative) intensities.

For the room-temperature structures (V*c*) and (V*d*), atoms C33 and C34, and (VII*c*) and (VII*d*), atom C30, *SHELXL*97 (Sheldrick, 2008) suggested twofold disorder models. For structure (IV*b*) a disorder model was recommended by *SHELXL*97 for C53 and/or C33, depending on the weight given to zero intensities. The crystal data in Table 1A (in the supplementary material) are for models without disorder.

4. Results: thermal motion analysis

4.1. Rigid-group test

*THMA*14*C* (Schomaker & Trueblood, 1998; Rosenfield *et al.*, 1978; Farrugia, 1999) differs from the earlier *THMA*11 in the treatment of correlations between 'attached rigid-group' (ARG) parameters and the rigid-body parameters of the entire molecule. All calculations are performed in the Cartesian crystal system. A goodness-of-fit agreement factor compares ΔU (defined as $U_{\rm calc} - U_{\rm obs}$) with e.s.d.s ($U^{ij}$) for a useful check on the model for both ARG and the rigid-body 'molecule'. Structural units to be treated as 'rigid bodies' should meet the Hirshfeld ΔMSDA test not only between bonded atoms but between *all* atoms. We have used either the whole molecule or a six-membered ring with its attached TBGs as the 'molecule', depending on rigidity.

To establish a realistic rigidity criterion, we may use as an example the crystal structure of (2,4,6-tri-*tert*-butyl-C_6H_2)P═P(2,4,6-tri-*tert*-butyl-C_6H_2) (II) (Cowley *et al.*, 1997), the phosphorus analogue of (I). Fig. 8 shows similar views of (II) and (I). Both structures were determined using Mo $K\alpha$ radiation at 100 K, but the high-precision structure of (II) was especially undertaken to distinguish bonding effects from thermal effects ($\theta_{\rm max} = 40^\circ$, multipole refinement), while the data for (I) extend only to $\theta_{\rm max} = 25^\circ$.

The results for (II) shown in Table 3 are from ADP analysis by *THMA*14*C*, using positions and ADPs from the full data refinement. The rigid-*bond* test is met fairly well (RMSΔ = 0.0016 Å^2 or 1.6 times MESDU). However, there are several rather large ΔMSDA values (including six values $\geq 4 \times$ MESDU, bold type). The *molecule* cannot be termed a 'rigid body' by the Hirshfeld test.

Four regions in Table 3 are italicized: three blocks of six ΔMSDA values for the three TBGs in the asymmetric unit and one block of 15 ΔMSDA values for the phenyl ring. The three underlined values in the TBG blocks are from quaternary to methyl C atoms, while the other three values are from methyl to methyl C atoms.

The following tests are imposed: MESDU $\leq$ 0.001 Å^2 *and* TBGR $\leq$ 3.0. In the convention of Table 3, in which ΔMSDA is shown in Å$^2 \times 10^4$, the TBGR for C15–C18 (lower left block) is $[(11^2 + 16^2 + 0^2)/3]^{1/2}/10$ or 1.1. All three of the independent TBGs in the molecule may be considered rigid by this test, with values of TBGR of 0.9, 1.7 and 1.1. The benzene ring also satisfies the rigidity test (RMSΔ/MESDU = 1.2).

Table 3 values are calculated for all X-ray data. If high-angle only positions and ADPs are used (data with $0.70 < \sin\theta/\lambda < 0.85$; Cowley *et al.*, 1997), RMSΔ (bonded) falls to 0.0006 Å^2, although RMSΔ for *all* atoms is approximately constant at 0.0040 Å^2. The results of thermal motion analysis appear in the next section.

4.2. ADP analysis with TBGs as ARGs

Table 4 presents thermal-motion analysis results for (II) (Cowley *et al.*, 1997). Libration amplitudes, $\langle\Phi^2\rangle$, are to be compared with the overall libration of the half-molecule of

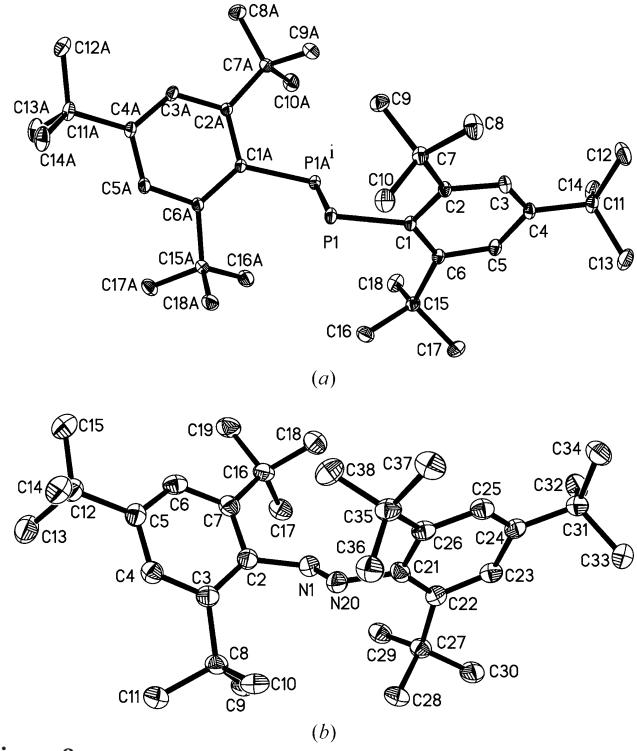

Figure 8
(*a*) Structure of compound (II) (Cowley *et al.*, 1997); atomic numbering and ellipsoids. The two halves of the molecule are related by a twofold axis [symmetry code: (i) $-x, y, -z + 1/2$, P1*A etc.*]. (*b*) A similar view of (I) (Table 1), which has no internal symmetry. H atoms omitted; ellipsoids enclose 50% probability.

Table 4
Thermal motion analysis with TBGs as ARGs for structure (II) (Cowley *et al.*, 1997).

ΔMSDA values as in Table 3; inter-methyl ΔMSDA in bold type. Results are also given for (I) for which only ΔMSDA (bonded) is shown. The calculated uncertainty in $\langle\Phi^2\rangle$ is in parentheses (*THMA*14*C*). Harmonic and torsional sixfold barriers (kJ mol^{-1}) are given for TBGs for which TBGR $\leq$ 3.0 and $\langle\Phi^2\rangle \geq$ 17 deg^2. See §4.2.4. Torsional barriers are rounded to the nearest kJ mol^{-1}.

	ΔMSDA			MESDU	GOF	TBGR	TBG type	Position	$\langle\Phi^2\rangle$ (deg^2)	Harmonic B-6	Torsional B-6
(II), all data											
C7	*20*	*6*	*22*	0.0010	2.01	0.9	*B–C*	*ortho*	11 (3)		
C8	***13***	***−6***									
C9	***6***										
C11	*29*	*33*	*17*	0.0010		1.7	*A–C*	*para*	17 (3)	9.9	10
C12	***19***	***23***									
C13	***−2***										
C15	*24*	*19*	*12*	0.0010		1.1	*C*	*ortho*	8 (2)		
C16	***−11***	***16***									
C17	***0***										
(II), high order											
C7	*2*	*5*	*6*	NA			*B–C*	*ortho*	9 (2)		
C8	***3***	***−10***									
C9	***7***										
C11	*2*	*5*	*−3*				*A–C*	*para*	19 (3)	8.6	9
C12	***1***	***−7***									
C13	***6***										
C15	*2*	*9*	*6*				*C*	*ortho*	5 (2)		
C16	***−9***	***5***									
C17	***4***										
(I) (Table 1)											
C8–C11	*44*	*−2*	*70*	0.0018	1.41	0.8	*C*	*ortho*	12 (4)		
C12–C15	*18*	*74*	*91*	0.0018		1.8	*A–C*	*para*	20 (4)	8.2	9
C16–C19	*44*	*38*	*22*	0.0018		2.3	*B—C*	*ortho*	7 (3)		
C27–C30	*53*	*73*	*19*	0.0017	1.35	1.0	*B–C*	*ortho*	5 (3)		
C31–C34	*4*	*30*	*25*	0.0017		1.3	*A–C*	*para*	20 (4)	8.2	9
C35–C38	*5*	*48*	*7*	0.0017		0.9	*B–C*	*ortho*	12 (3)		

3.3 (3) deg^2. Refinement with high-order data only reduced ΔMSDA values, especially the bonded (underlined) values, but did not significantly change $\langle\Phi^2\rangle$ [no e.s.d. (U^{ij}) was given]. The *ortho* TBGs are not 'moving' at 100 K, perhaps due to crowding, but $\langle\Phi^2\rangle$ of the *para* TBG is 5–6 times the overall L11 value, and more than 6 times L11 in the ARG direction (2.5 deg^2). The precision of $\langle\Phi^2\rangle$ values in Table 4 is further reduced because they include the unknown correlation term, $2\varphi\lambda^{\parallel}$ (see §2.1).

Values for $\langle\Phi^2\rangle$ for (I), calculated for each half-molecule after the refinement summarized in Table 1, are also shown. Libration amplitudes for (I) at both the *ortho* and *para* positions are similar to those for (II). TBGR is satisfactory given the reduced precision of the refinement; Fig. 8 shows the difference in ADP *magnitude* between the two 100 K structures!

Table 5 gives ADP analysis results for (III*a*), (V*a*) and (VII*a*), the three new structures in this work that satisfy both of the tests: MESDU $\leq$ 0.0010, TBGR $\leq$ 3.0.

Some TBGs from structures (III*b*), (IV*a*), (V*b*), (V*c*) and (VII*b*) are included for comparison.

4.2.1. Libration amplitudes for TBGs as ARGs. All $\langle\Phi^2\rangle$ values for *ortho* TBG groups in Tables 4 and 5 are small compared with L11 (overall libration of the 'molecule') or with their precision. TBGR values for the TBG C31–C34 in (V*a*) suggest that the TBG is *not rigid* (*i.e.* Me groups, especially C33, may be moving independently). There may be disorder or the ADPs may be affected by the impurity (Fig. 5, Table 1) in the crystal.

4.2.2. Model for rigid body and ARGs. The model for the 'molecule' in (III) is a six-membered ring with the TBGs as ARGs (18 atoms for rings C3–C8 and C3*B*–C8*B*, 14 atoms for ring C9–C14, and 10 atoms for ring C9*B*–C14*B*, disordered TBG omitted). Similarly for (IV), the 'molecule' is 14 atoms, while for (V) the hexahelicene with 2 ARGs totals 34 atoms.

The effect of a choice of model can be dramatic. When the TBG C27–C30 in (VII*a*) is treated as an ARG attached to the rest of the molecule (assumed to be rigid), the amplitude of libration of the ARG is larger than in two other tested models. As seen in Fig. 7, the benzene ring also appears to be 'moving' with respect to the tetrahelicene portion of the molecule; if the 10-atom portion (benzene ring plus TBG) is treated as a 'molecule' with the TBG as an ARG, the calculated $\langle\Phi^2\rangle$ for the ARG decreases to 8 deg^2. Agreement factors such as the goodness-of-fit (GOF) improve (1.39 *versus* 2.89). Alternatively, the entire molecule may be used with a 2-ARG model; *tert*-butylphenyl as one ARG and the TBG as another (model 2 in Table 5). All three of these models give the same bond length corrections for the TBG while $\langle\Phi^2\rangle$ for the TBG varies from 8 to 45 deg^2. See further discussion in §4.6.

For the TBGs in which one C_{Me} has a large displacement amplitude a model downweighting that atom was tested; $\langle\Phi^2\rangle$

Table 5
Thermal motion analysis with TBGs as ARGs for structures (III*a*), (IV*a*), (V*a*) and (VII*a*).

Results for some TBGs in (III*b*), (V*b*), (V*c*) and (VII*b*) are shown for comparison. TBGRO = overall TBGR, including bonded atoms. Harmonic and torsional sixfold barriers (kJ mol^{-1}) are given for TBGs for which TBGR $\leq$ 3.0 and $\langle\Phi^2\rangle \geq 17$ deg^2. See §4.2.4. Torsional barriers are rounded to the nearest kJ mol^{-1}.

Structure	*T* (K)	MESDU	GOF	TBGR	TBGRO	TBG TYPE	Position	$\langle\Phi^2\rangle$ (deg^2)	Harmonic B-6	Torsional B-6
(III*a*) (Fig. 2)	100									
C17–C20		0.0006	1.74	1.0	1.8	*C*	*ortho*	6 (1)		
C21–C24		0.0006		2.0	2.3	*A–C*	*para*	5 (2)		
C25–C28		0.0006		1.0	1.1	*C*	*ortho*	4 (1)		
C29–C32		0.0006	1.88	2.5	4.4	*A–C*	*meta*	52 (2)	3.0	4
C33–C36		0.0006		1.2	3.4	*A–C*	*meta*	22 (2)	7.5	8
C17*B*–C20*B*		0.0006	1.77	2.0	2.0	*C*	*ortho*	9 (2)		
C21*B*–C24*B*		0.0006		0.3	2.5	*A–C*	*para*	20 (2)	8.2	9
C25*B*—C28*B*		0.0006		1.3	1.7	*C*	*ortho*	1 (1)		
C29*B*–C32*B*		0.0008	2.15	0.9	2.0	*C*	*meta*	29 (3)	5.5	6
(III*a*) high order	100									
C29–C32		0.0007	1.93	2.5	1.9	*A–C*	*meta*	53 (3)	3.0	4
C33–C36		0.0007		2.1	2.0	*A–C*	*meta*	21 (3)	7.8	8
C21*B*–C24*B*		0.0006	2.03	0.6	1.3	*A–C*	*para*	20 (2)	8.1	9
C29*B*—C32*B*		0.0010	1.76	0.4	0.3	*C*	*meta*	38 (3)	4.2	5
(III*b*)	145									
C29–C32		0.0035	1.33	1.9	1.6	*A–C*	*meta*	73 (9)	3.0	5
C33–C36		0.0035		3.9	3.8	*A–C*	*meta*	45 (9)		
C21*B*–C24*B*		0.0035	1.25	3.1	2.6	*A–C*	*para*	35 (7)		
C29*B*–C32*B*		0.0035	1.07	2.9	2.7	*C*	*meta*	57 (10)	3.9	6
(IV*a*)	128									
C31–C34		0.0014	1.74	2.2	2.9	*A*	*meta*	35 (3)	5.7	7
C51–C54		0.0014		2.4	2.7	*A*	*meta*	41 (4)	4.9	6
C31–C34 (model 2)†		0.0014	NA			*A*	*meta*	37 (5)	5.5	7
C51–C54†		0.0014				*A*	*meta*	40 (7)	5.1	6
(V*a*) (Fig. 5)	100									
C27–C30		0.0007	3.00	1.3	2.1	*A*	*meta–para*	18 (3)	9.4	9
C31–C34		0.0007		8.8	7.3	*A*	*meta–para*	88 (4)		
(V*a*) high order	100									
C27–C30		0.0010	2.57	1.1	1.1	*A*	*meta–para*	18 (2)	9.4	9
C31–C34		0.0010		6.9	4.9	*A*	*meta–para*	84 (5)		
(V*b*) Cu *Kα*	100									
C27–C30		0.0007	3.72	0.7	2.7	*A*	*meta–para*	18 (3)	9.4	9
C31–C34		0.0007		9.2	8.2	*A*	*meta–para*	86 (5)		
(V*c*) Mo *Kα*	298									
C27–C30		0.0013	4.52	1.3	3.3	*A*	*meta–para*	84 (8)	5.4	8
(VII*a*)	100									
C27–C30		0.0008	2.89	2.5	3.4	*C*	*para*	45 (4)	3.5	5
C27–C30 (model 2)‡		0.0008	2.57					26 (5)	6.3	7
(VII*a*) high order										
C27–C30		0.0010	2.43	2.5	2.1	*C*	*para*	46 (4)	3.4	5
C27–C30 (model 2)‡		0.0010	2.16					27 (5)	6.0	7
(VII*b*) Cu *Kα*	100									
C27–C30		0.0006	3.98	3.9	5.2	*C*	*para*	46 (4)		

† C33 and C53 downweighted (atoms with largest ADPs). See §4.2.2. ‡ Two ARGs: *p-tert*-butylphenyl plus C27–C30 TBG. See §4.2.2.

was not strongly affected. Since this model uses artificial e.s.d.s (U^{ij}) for the downweighted atom, GOF is not applicable.

4.2.3. Improvement in ADPs by omitting low-angle data in refinement. Table 4 displays a very common feature of ΔMSDA values for TBGs: the mean ΔMSDA along the bonding directions (underlined in Tables 3 and 4) is generally larger than the mean ΔMSDA along the *methyl–methyl* directions (bold in Table 4). However, if only higher-order data are used to refine ADPs for structures (II), (III*a*), (V*a*) and (VII*a*) (Tables 4 and 5) ADPs are reduced in magnitude and ΔMSDA is improved for all the bonded atoms in the TBGs. Libration amplitudes are not strongly affected. An exception is $\langle\Phi^2\rangle$ for C29*B*–C32*B* in (III*a*), for which L11 in the direction of the ARG axis is large, about 12 deg^2.

4.2.4. Barriers to torsional motion. Calculated barriers for TBGs with sufficiently precise $\langle\Phi^2\rangle$ values are shown in Tables

4 and 5. Some higher-temperature values, and Cu $K\alpha$ (100 K) results for (V*b*), are also given. Threefold and sixfold harmonic barriers are calculated by *THMA*14*C* using a quadratic approximation to the *n*-fold sinusoidal potential $V(\varphi) = B(1 - \cos n\varphi)/2$. In this approximation, valid for small values of φ, the potential is a quadratic function of φ. The further approximation (§2.1) $\langle\Phi^2\rangle \sim \varphi^2$ gives the harmonic barrier $B = 2RT/n^2\langle\Phi^2\rangle$. For a given value of $\langle\Phi^2\rangle$, threefold harmonic barriers ($n = 3$) are four times as large as sixfold harmonic barriers ($n = 6$).

The sixfold torsional barriers, calculated from $V(\varphi) = B(1 - \cos 6\varphi)/2$ by Boltzmann averaging, are higher than the corresponding harmonic barriers as $\langle\Phi^2\rangle$ increases. Most $\langle\Phi^2\rangle$ values for these structures are too small to permit calculation of precise threefold torsional barriers; the sixfold barriers range from about 4 to about 10 kJ mol^{-1}. Fig. 4B in the supplementary material gives a plot of torsional barriers for the range $\langle\Phi^2\rangle$ = 0–100 deg^2 (Maverick *et al.*, 1991; Maverick & Dunitz, 1987).

The two (III*b*) *meta* TBGs that meet the TBGR criterion at 145 K give nearly the same torsional barriers as at 100 K, showing the expected temperature dependence of $\langle\Phi^2\rangle$. The (V*c*) TBG that meets the TBGR criterion at 298 K gives a torsional barrier of 8.5 kJ mol^{-1}. The latter value is reduced by $\sim$10% from the value at 100 K (9.4 kJ mol^{-1}).

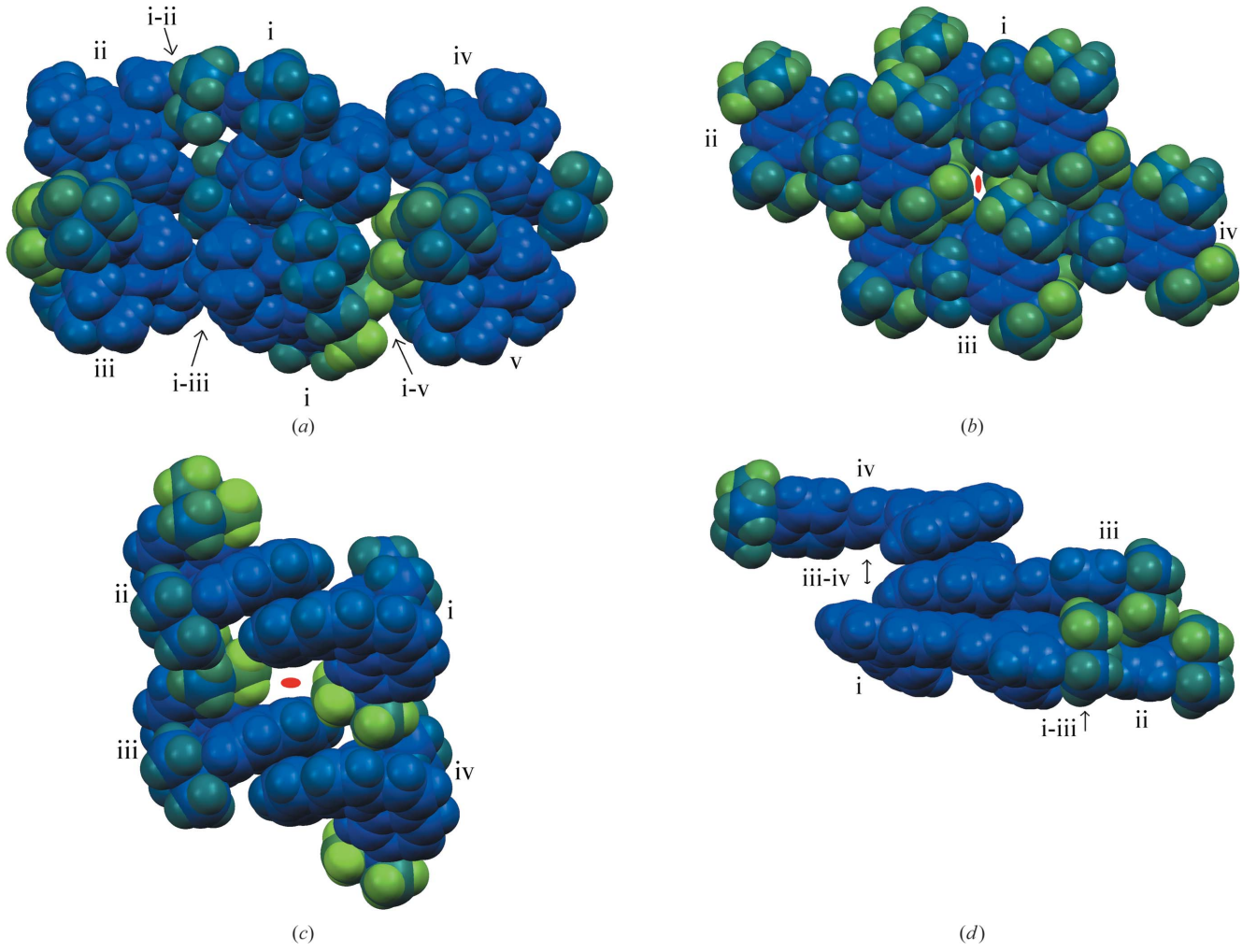

Figure 9
Spacefill diagrams (CSD Mercury; Macrae *et al.*, 2008) showing short and long intermolecular distances for structures (III*a*), (IV*a*), (V*a*) and (VII*a*). (*a*) Six molecules of (III) in (III*a*). The view is approximately the same as in Fig. 3. Symmetry codes: (i) x, y, z; (ii) molecule 1, $-x+1, -y+1, -z$; (iii) molecule 2, $-x+2, -y+1, -z$; (iv) molecule 1,$-x+1, -y+2, -z+1$; (v) molecule 2, $-x+2, -y+2, -z+1$. Colours by atomic displacement; the lightest green atoms are in the disordered TBG (C33*D*–C36*D*; only the major conformer is shown). The close contact between molecule 2, position i, and molecule 2, position iii, is indicated by an arrow, as are the 'gaps' i–ii and i–v. (*b*) Four molecules of (IV) in structure (IV*a*). Symmetry codes: (i) x, y, z and $-x+1, -y+1, -z+2$; (ii) $x+1, y, z$ and $-x+2, -y+1, -z+2$; (iii) $x+1, y, z-1$ and $-x+2, -y+1, -z+1$; (iv) $x, y, z-1$ and $-x+1, -y+1, -z+1$. Distances across the centre at 1, $\frac{1}{2}$, $\frac{1}{2}$, indicated by a red oval: C33$^{i}\cdots$C33^{iii}, 5.95 Å and C53$^{ii}\cdots$C53^{iv}, 6.91 Å. (*c*) Four molecules of (V) in (V*a*), showing $\pi\cdots\pi$ stacking. Symmetry codes: (i) x, y, z; (ii) $-x+1, -y+2, -z+1$; (iii) $-x, -y+2, -z+1$; (iv) $x-1, y, z$. Centre at 0, 1, $\frac{1}{2}$ indicated by a red oval; C33$^{i}\cdots$C33^{iii} distance = 5.98 Å. (*d*) Four molecules of (VII) in (VII*a*), showing $\pi\cdots\pi$ stacking distance, C15$^{iii}\cdots$C20^{iv} = 3.27 Å across the centre; C—H$\cdots\pi$ distance H30*C*$^{i}\cdots$C4^{iii}, 3.15 Å. Symmetry codes: (i) x, y, z; (ii) $x, y, z-1$; (iii) $x, -y+\frac{1}{2}, z-\frac{1}{2}$; (iv) $-x+1, y+\frac{1}{2}, -z+\frac{3}{2}$. The *b* axis is approximately vertical in this view.

Table 6
Results of packing calculations (Gavezzotti, 2003) for low-temperature structures (III*a*)–(VII*a*).

Structure	Formula	Formula weight	T (K)	Molecular volume (Å^3)	Molecular surface area	d (g cm^{-3})	Packing coeff.	$\Delta H_{\rm sublim}$ (kJ mol^{-1})
(III*a*) mol. 1	$C_{36}H_{58}$	490.82	100	541	580	1.015	0.674	−302.8 (2 mols)
(III*a*), mol. 2	$C_{36}H_{58}$	490.82		541	581			
(III*b*), mol. 1	$C_{36}H_{58}$	490.82	145	541	580	1.005	0.668	−300.4 (2 mols)
(III*b*), mol. 2	$C_{36}H_{58}$	490.82		542	584			
(IV*a*)	$C_{36}H_{58}$	490.82	128	539	604	0.997	0.660	−176.5
(V*a*)	$C_{34}H_{32}$†	430.1	100	433	456	1.190	0.704	−164.2
(VII*a*)	$C_{30}H_{26}$	386.51	100	380	415	1.222	0.723	−195.1

† Iodine removed for this calculation.

4.3. Packing analysis for (III*a*), (III*b*), (IV*a*), (V*a*) and (VII*a*)

Packing for the five low-temperature hydrocarbon structures was analyzed using *OPiX*, a computer program for the calculation of intermolecular interactions (Gavezzotti, 2003). Table 6 presents the results of calculation of molecular volume and surface area by the method of spheres & caps, and the enthalpy of sublimation using an exp-6 force field (Gavezzotti & Filippini, 1994). Fig. 9 shows some features of interest.

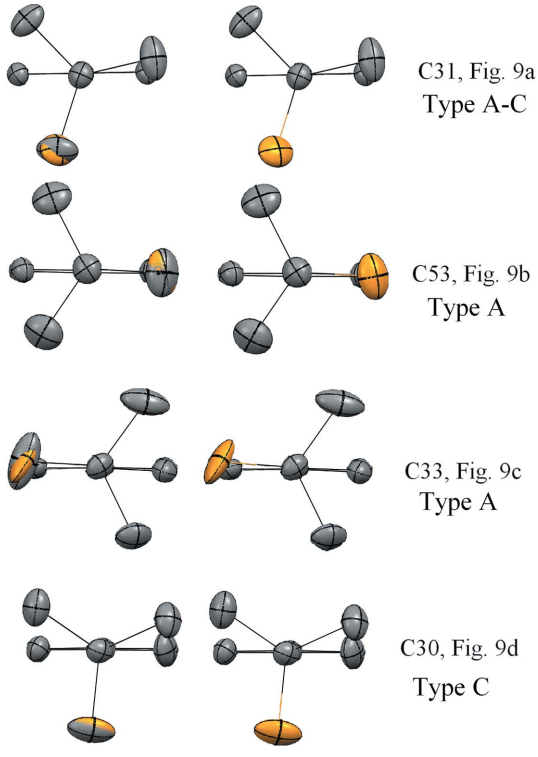

Figure 10
TBG methyl groups with large displacement amplitudes, showing ellipsoids from calculated and observed ADPs. Calculated ADPs were obtained by downweighting the C_{Me} with the largest displacements (Table 5). Orange ellipsoids use calculated ADPs for the downweighted C_{Me}; gray ellipsoids use observed ADPs. (Left, both observed and calculated ADPs are shown; right, only calculated ADPs are shown for the downweighted C_{Me}.) In the first three TBGs the orange (calculated) ellipsoid is smaller, with a different orientation. In the fourth (Type *C*), size and orientation are more nearly equal. ADPs for (III*a*), (V*a*) and (VII*a*) taken from high-order refinements (Table 5, 100 K); (IV*a*), Table 5 (128 K).

For (III*a*) the strongest destabilizing interaction is the short distance (3.30 Å) between C28*B*$^{\rm i}$ and C28*B*$^{\rm iii}$ (Fig. 9*a*), 40 kJ mol^{-1} in this force field, in keeping with the very small $\langle\Phi^2\rangle$ for TBG C25*B*–C28*B* (Table 5). There is a stabilizing C—H···C intermolecular interaction between C9 and H16*E*, −6 kJ mol^{-1} (*OPiX* lengthens C—H bond distances to 1.08 Å). Related C16–centroid C9*B*—C14*B* and C16*B*–centroid C9—C14 distances of ∼ 3.5 Å are given in Table 3A of the supplementary material. Zeller *et al.* (2009) shows a similar C_{Me}–aromatic centroid intermolecular distance, 3.50 Å.

As Fig. 9(*a*) shows, there are 'holes' in the packing that suggest an explanation for the disorder of the TBG at C33*B*–C36*B*,*D* [occupancies 0.080 (3)/0.920 (3)] and the relatively large thermal motion of the TBG at C29–C32 (see Table 5). Thus (III*a*) fits the description of a structure with two molecules in the asymmetric unit as a crystal in the making, with some intermolecular distances too short and some too long to be at equilibrium (Desiraju, 2007). For (III*b*), at 145 K, volume and surface area are slightly larger for molecule *B* (major conformer) and the packing coefficient is slightly smaller.

Structure (IV*a*) has the lowest packing coefficient of the four hydrocarbons. No intermolecular contacts are found with distances less than the sum of the van der Waals radii. The *meta* TBGs, especially C33 and C53, have the largest displacement amplitudes in the structure, and there is a 'hole' in the packing between these atoms and those related by a centre of symmetry (Fig. 9*b*). Although the TBGs are Type *A*, there is evidence that C33 and C53, the in-plane methyls, are 'moving' with a greater amplitude than C32, C34 and C52, C54.

In the *OPiX* force field the $\pi\cdots\pi$ stacking distance in structure (V*a*) (C7$^{\rm i}\cdots$C26$^{\rm ii}$ = 3.32 Å) gives a net interaction energy of 0 kJ mol^{-1}. The packing coefficient is greater than those of structures (III) and (IV). Calculations (Table 6), and the drawing in Fig. 9(*c*), omit the low-occupancy iodine atoms. The displacement amplitude for C33 is very large (Fig. 9*c*), perhaps owing to a 'hole' across a centre of symmetry.

More extensive $\pi\cdots\pi$ interactions are found in (VII*a*), which has the highest packing coefficient of the four structures. The *OPiX* force field finds destabilizing energies for short distances (C15$^{\rm iii}\cdots$C20$^{\rm iv}$, Fig. 9*d*, gives a net interaction energy of 0.1 kJ mol^{-1}) and there are no H···H or H···C distances less than the sum of the van der Waals radii. The

Table 7
Summary of ADP analysis for search results [CSD Version 5.29 (November 2007, database April 2009) total hits, 76]; includes only hits with MESDU ≤ 0.001 Å^2 [47 hits in all; 7 TBGs excluded on rigidity criterion, 2 others excluded due to very large RMSΔ (bonded) values].

Table 7B (summary of TBG ARG analysis of CSD entries) and Table 7C (rigidity and $\langle\Phi^2\rangle$ for CSD entries, by TBG type) are found in the supplementary material.

TBG type	No. of TBGs, TBGR ≤ 3.0	Range of $\langle\Phi^2\rangle$ (deg^2)	Average $\langle\Phi^2\rangle$ (deg^2) (ave. dev.)	B-6 (kJ mol^{-1}) for average $\langle\Phi^2\rangle$
A	34	0–36.9	20.2 (7.5)	8
B	35	0–39.5	12.6 (7.2)	14
C	19	5.1–33.0	17.8 (7.4)	9
TBG type (structures containing C, H, N, O only)				
A	27	0–36.2	20.6 (6.7)	8
B	18	0–39.5	14.5 (8.1)	11
C	14	5.2–33.0	19.2 (7.0)	9
TBG type (hydrocarbons only)				
A	7	0–36.2	15.8 (11.7)	11
B	0	NA	NA	NA
C	8	5.2–18.9	13.7 (3.4)	12
TBG type (hydrocarbons only, omit *p-tert*-butylphenyl)				
A	3	1.3–36.2	15.0 (14.1)	11
C	2	8.6–13.1	13.4 (4.8)	12

'perpendicular' conformation of the TBG C27–C30 (Fig. 1), and the relatively short C—H···C distances involving TBG H atoms (Fig. 9*d*) suggest C—H···π interactions.

Finally, we have explored the suggestion (large ADPs, no short intermolecular interactions) that some Me groups in the TBGs may exhibit additional motion. Fig. 10 shows the results of downweighting the C_{Me} with large ADPs (Fig. 9*a–d*). [Note that the third TBG (C33) in Fig. 10 does not meet the TBGR test.]

The calculated ADPs differ in magnitude and orientation from those observed, perhaps due to low-barrier methyl motion in the small voids in the crystals.

4.4. ADP analysis with TBGs as ARGs: search results, Cambridge Structural Database

The Cambridge Structural Database (Allen, 2002; Bruno *et al.*, 2002) was searched with the following queries: structural motif, TBG attached to a six-membered aromatic ring; T = 100 K; X-rays; R factor ≤ 0.075; only organics; not disordered; no ions; no powder structures; no errors. Thermal motion analysis used *THMA*14*C*. The first model employed was the entire molecule, excluding solvent, with each TBG as an ARG librating about the axis defined by the $C_{Ar}—C_t$ bond. Two or more molecules in the asymmetric unit were analyzed separately. Barriers were calculated with the harmonic model. In the analysis, 1/e.s.d. (U^{ij}) was used to weight the U^{ij} values.

Table 7 gives the results of ADP analysis of the recovered structures. Over 60% of the structures meet the MESDU test. The range of calculated $\langle\Phi^2\rangle$ (Schomaker & Trueblood, 1998) is large for all three types of TBG. Precision and goodness-of-fit are often poor. Nevertheless, this model gives an estimate of the motion of the TBG with respect to the molecule as a whole, and yields bond length corrections for bonds within the TBG.

Better goodness-of-fit may be obtained by treating each aromatic unit with attached TBG(s) as an independent molecule with TBG as ARG. This change in model can give more precise $\langle\Phi^2\rangle$ values. For example, a supermesityl phosphoquinone (Sasaki *et al.*, 1999) gives $\langle\Phi^2\rangle$ = 37 (6) deg^2 for *p*-TBG, GOF = 4.80, for the whole-molecule model, and $\langle\Phi^2\rangle$ = 24 (2) deg^2 for the *p*-TBG, GOF = 1.52, if the supermesityl group is treated alone. The latter $\langle\Phi^2\rangle$ value is similar to those obtained for the same group in (II) and (I) (Table 4).

However, if the 'molecule' is a benzene ring with a *para* TBG attached (total of 10 atoms), the additional motion of the TBG is always reduced, often to zero. The benzene ring librates about the same axis, ADPs for ring atoms are more heavily weighted in the analysis than TBG methyl atoms, and the libration of the ring is strongly correlated to that of the TBG ARG. This phenomenon is seen in the analysis of (VII*a*), and in the recovered calixarenes in the CSD sample. (More detail is given in Tables 7B and 7C in the supplementary material.)

The variation in calculated $\langle\Phi^2\rangle$ for the recovered structures is wide. Still, since the ranges and average deviations of the values are comparable for the three types, on average Type *B* TBGs ('planar', with an *ortho* substituent on the aromatic ring) have smaller ADP ellipsoids, and thus higher calculated barriers to torsional motion than Type *A* or Type *C* TBGs.

In the *hydrocarbons* (Table 7), as in the structures in this paper, there are no true Type *B* TBGs. Only 1 of a total of 15 TBGs is in an *ortho* position (9-*tert*-butylanthracene; Angermund *et al.*, 1985), and it is bent out of plane and 'perpendicular' in conformation (Type *C*, Fig. 1*b*). Of the other 7 Type *C* TBGs one is in a *meta* and 6 are in *para* positions.

4.5. ADP analysis with TBGs as ARGs: Comparison with results from dynamical nuclear magnetic resonance studies

Table 8 presents the results of thermal motion analysis for the crystal structures reported by Beckmann and co-workers (Beckmann, 1981; Beckmann *et al.*, 1988, 1994, 2000, 2003, 2004, 2009; Fry *et al.*, 1991), for comparison with the reorientation barriers determined by nuclear-spin relaxation studies. All of these studies involve TBG substituents in aromatic molecules.

Only three $\langle\Phi^2\rangle$ values from ADP analyses are large enough for precise calculation of barriers, the *B* and *C* molecules of 2-*tert*-butylanthracene (2TA), with Cu $K\alpha$ radiation and three molecules in the asymmetric unit, and 4,5-

Table 8
Comparison of barriers to TBG reorientation determined by solid-state NMR spin-lattice relaxation studies with those calculated from ADPs from the corresponding crystal structures.

								Calculated barriers (kJ mol^{-1})			
Compound	T (K)	Θ_{max}	Source	MESDU	TBGR	$\langle\Phi^2\rangle$ (deg^2)	Type	Sixfold (harm.)	Sixfold (tors.)	Threefold (harm.)	NMR
2,6-DTN†	223	28.52	Mo $K\alpha$	0.0015	0.4	12 (7)	*A*	30	29	120	18
2TA (*A*)‡	100	68.31	Cu $K\alpha$	0.0015	1.0	0	*A–C*	∞	∞	∞	25
2TA (*B*)	100			0.0015	1.6	17 (3)	*A–C*	10	10	39	21
2TA (*C*)	100			0.0015	1.2	17 (3)	*A–C*	10	10	41	21
2TAQ (*A*)§	100	69.08	Cu $K\alpha$	0.0016	3.6	7 (4)	*A*	29	23	115	16
2TAQ (*B*)	100			0.0015	1.2	1 (4)	*A*	∞	∞	∞	16
TMP (*A*)¶	173	26.0	Mo $K\alpha$	0.0007	1.7	7 (4)	*B*	44	40	178	32
TMP (*B*)	173			0.0007	1.8	7 (4)	*B*	42	37	166	30
TMP (*B*)††	173			0.0007	1.8	14 (4)	*B*	20	12	80	30
3TBC‡‡	173	22.5	Mo $K\alpha$	0.0020	2.1	10 (6)	*A*	28	27	111	24
TBBrX§§	100	28.19	Mo $K\alpha$	0.0010	2.4	27 (4)	*A*	6	7	24	17
TBBrX††	100			0.0010	2.4	16 (5)	*A*	10	10	42	17
TBBrX¶¶	100			0.0010	2.4	30 (4)	*A*	6	6	22	17

† 2,6-Di-*tert*-butylnaphthalene (Beckmann *et al.*, 2000); CCDC 144219. ‡ 2-*tert*-Butylanthracene (Rheingold *et al.*, 2008); three molecules in the asymmetric unit; CCDC 675773. § 2-*tert*-Butylanthraquinone (Rheingold *et al.*, 2008); two molecules in the asymmetric unit; CCDC 675772. ¶ 2-*tert*-Butyl-4-methylphenol (Beckmann *et al.*, 2004); two molecules in the asymmetric unit; CCDC 250114. †† 10-atom model; see text. ‡‡ 3-*tert*-Butylchrysene (Beckmann *et al.*, 2003); CCDC 156308. In Beckmann *et al.* (2004) it is suggested that in 3TBC (Type *A* TBG) one Me group may reorient with a different barrier than the other two. §§ 4,5-Dibromo-2,7-di-*tert*-butyl-9,9-dimethylxanthene (Beckmann *et al.*, 2009); CCDC 699537. ¶¶ TBBrX, analyzed with 2 ARGs, no correlations, $\langle\Phi^2\rangle$ calculated from C8 and C10. See text.

Table 9
Bond-length corrections (*THMA*14*C*) for four TBGs of different types.

The contributions of ARG motion and parallel 'molecular' motion are shown. Distances in Å, angles in °.

C_t	C_{Me}	Distance	Corrected distance	Total correction	Correction, parallel motion	Correction, ARG	Angle, $C_{Ar}-C_t-C_{Me}$	$\langle\Phi^2\rangle$ (deg^2)	$\langle\Phi^2\rangle$ (deg^2) No correlations
(III*a*), high order, Type *A–C*									
C29	C30	1.5335	1.546	0.0123	0.0018	0.0105	112.4 almost in-plane	53	50
C29	C31	1.5374	1.551	0.0131	0.0021	0.0110	108.9		
C29	C32	1.5376	1.550	0.0123	0.0015	0.0108	110.7		
(V*a*), high order, Type *A*									
C27	C28	1.5346	1.539	0.0045	0.0008	0.0037	108.5	18	18
C27	C29	1.5392	1.544	0.0047	0.0011	0.0037	109.5		
C27	C30	1.5302	1.535	0.0048	0.0013	0.0035	112.5 in plane		
(VII*a*), 10-atom model (phenyl plus TBG), Type *C*									
C27	C28	1.5323	1.542	0.0100	0.0083	0.0017	111.5	8	8
C27	C29	1.5314	1.542	0.0108	0.0091	0.0017	111.4		
C27	C30	1.5309	1.542	0.0110	0.0092	0.0018	107.8 perpendicular		
TMP, (*B*) (Table 8), 10-atom model (phenyl plus TBG), Type *B*									
C7′	C8′	1.5404	1.547	0.0063	0.0030	0.0033	109.8	14	14
C7′	C9′	1.5285	1.536	0.0077	0.0046	0.0032	112.1 in plane		
C7′	C10′	1.5369	1.544	0.0074	0.0041	0.0033	110.2		

dibromo-2,7-di-*tert*-butyl-9,9-dimethylxanthene (TBBrX). For 2TA, molecules *B* and *C*, and for TBBrX, the NMR barrier lies between the threefold and the sixfold ADP-calculated barriers.

Two crystal structures, 2-*tert*-butyl-4-methylphenol (TMP) and TBBrX, meet both the MESDU and the TBGR tests. The calculated $\langle\Phi^2\rangle$ values are highly model-dependent. For TMP, $\langle\Phi^2\rangle$ is greater when the 10-atom model (the *tert*-butylphenyl group) is used, although the value is small compared with its calculated precision. For TBBrX, $\langle\Phi^2\rangle$ is smaller with the 10-atom model, which also consists of the *tert*-butylphenyl moiety.

For TBBrX, as for 3-*tert*-butyl-chrysene (3TBC), the NMR analysis proposes that two of the methyl groups in the Type *A* TBG reorient with the same barrier, while the third Me is different (Beckmann *et al.*, 2004, 2009).

Therefore, a crude model was tried for the 'different' Me group. In some structures, the in-plane Me group has the largest U_{equiv} value of the three [see Fig. 10 for examples from structures (IV*a*) and (V*a*)]. In TBBrX, however, the U_{equiv} values for the TBG Me C atoms are the same for C8 and C10 [0.0304 (6) Å^2], while that for C9, the in-plane Me, is 0.0239 (5) Å^2. The 2-ARG model for the TBG consists of a two-atom ARG (C8, C10) and a one-atom ARG (C9), both with the same libration axis (C4–C7). For the two-atom ARG, representing TBG rotation, $\langle\Phi^2\rangle$ = 30 (4) deg^2, while for the one-atom ARG $\langle\Phi^2\rangle$ = 14 (6) deg^2. This calculation must be

made with no correlations (Schomaker & Trueblood, 1998). The results are shown in the last line of Table 8.

4.6. Bond-length corrections for TBGs with planar and non-planar conformations

Although the ADPs, judged visually and by the Hirshfeld tests, may suggest that the TBG is a rigid body, the usual geometry of the TBG (in-plane C_t-C_{Me} distance shorter than the other two; in-plane $C_{Ar}-C_t-C_{Me}$ angle larger than the other two) means that reorientation would require adjustment of these distances and angles. Table 9 gives these distances, their thermal-motion corrections, and angles for four TBGs of different types. Table 9B in the supplementary material gives more examples.

*THMA*14*C* allows a choice of calculation of thermal motion parameters 'with correlations' (see §§2.1 and 4.2) or 'no correlations' (Schomaker & Trueblood, 1998). In both cases, the program subtracts the libration amplitude of the 'molecule' parallel to the ARG axis from $\langle\Phi^2\rangle$, and ignores correlations in calculating corrected bond lengths. The two 'correction' columns in Table 9 show contributions to bond-length corrections from parallel overall motion and from ARG motion. (For these TBGs, $\langle\Phi^2\rangle$ values are not significantly affected by the inclusion of correlations; see the last two columns of Table 9.)

For the examples of Types *A*, *A*–*C* and *B*, the in-plane C_t-C_{Me} distance is 0.004–0.012 Å shorter than the other two. Resonance stabilization may account for the difference, while the larger bond angle may lessen H···H repulsion. For (VII*a*), a Type *C* TBG, bond distances and angles are more nearly equal. For C29–C32 from (III*a*), nearly 90% of the correction is due to ARG motion. For (V*a*), C27–C30, the contribution from ARG motion is smaller (about 77%). For (VII*a*), $\langle\Phi^2\rangle$ is model-dependent and the parallel motion of the 'molecule' contributes strongly to the distance correction. For TMP (molecule *B*) the contributions of the ARG and of the parallel motion are nearly equal. Thus $\langle\Phi^2\rangle$, and the barrier calculated from it should be more precise for (III*a*), C29–C32, than for the other TBGs in Table 9.

5. Conclusions

5.1. The TBG substituent in aromatic compounds poses several problems for ADP thermal motion analysis.

In §1 two questions were asked, to describe the goals of this work. 'The ADP ellipsoids of *tert*-butyl groups in crystal structures are often elongated, suggesting motion or disorder in the solid state. Can a reasonable model for motion be fitted to the ellipsoids?'As seen in §4.2 there are often *several* models which give a good fit to the ellipsoids, but precision is usually low and analysis with torsional or harmonic models for the motion can give widely varying results.

First, crowded *ortho* TBGs in the new hydrocarbons (III) and (VI), even more than in the supermesityl compounds (I) and (II), are bent out of the aromatic plane, with an accompanying distortion of the ring. These TBGs show very little motion at 100 K. On the other hand, the *meta* and *para* TBGs with low calculated reorientation barriers in (III) and (V) may be affected by the distortion of the rings, while in (VII) the TBG is not in the lowest-energy 'planar' configuration (Fig. 1).

In addition, reorientation would require adjustment of distances and angles in the TBG (§4.6). In the TBG in (VII), with a 'perpendicular' conformation, the atypical distances and angles (Table 9) may represent the effects of a 30° rotation from a 'planar' minimum, combined with C—H···π attraction (§4.3, Fig. 9*d*).

5.2. At the low temperatures at which the Hirshfeld tests are met, ADP analysis yields amplitudes of libration that are too small and/or too strongly correlated to other modes for a precision comparable to that achieved in published NMR analysis.

'Does the model deduced from the crystal structure lead to agreement with other methods of measuring such motion?' The answer to the second question from §1 is 'no'. For the structures tested in §4.5, NMR barriers to reorientation of 16–32 kJ mol^{-1} (Table 8) are more precise than barriers calculated by ADP analysis from the corresponding published crystal structures. The NMR barrier values for the most precise structures are higher than sixfold barriers calculated from the ADPs (Table 8). These results show that the simple torsional model for the motion is inadequate.

Yet peaks in difference maps and highly oblique ADP ellipsoids often demonstrate that the TBG is best represented, at least at higher temperatures, by a disorder model, suggesting a sixfold (or higher) rotation of the group. A wide 'well' (*i.e.* low calculated barrier) from ADP analysis may suggest that sixfold rotation produces a higher-energy conformer. Such a model was proposed for the *para* TBG in (I) (Maverick *et al.*, 1991).

5.3. There is evidence, both from ADP analysis and from NMR results, that solid-state TBGs are not rigid.

The structures presented here suggest that even TBGs that satisfy the TBGR test may demonstrate additional motion of one or two of the constituent methyl groups. Such motion should not be ignored, but is difficult to model. As in the motion of other groups in the solid state (Khuong *et al.*, 2007, and references therein), barriers to reorientation may depend mainly on non-bonded interactions in the crystal.

ADP and packing analysis can help to identify which TBGs in a complicated structure reorient with lower barriers, and can also identify variations among the TBG methyl groups.

We thank Louis Farrugia for the *WinGX* version of *THMA*14*C* and his patience in correcting errors, the Cambridge Structural Database for the archiving of crystal structures from all over the world, the National Science Foundation for funding the early stages of this work, and the UCLA Molecular Instrumentation Center, partially funded by the California Nanosystems Institute, for X-ray crystallography.

References

Allen, F. H. (2002). *Acta Cryst.* B**58**, 380–388.
Anderson, J. E., Franck, R. W. & Mandella, W. L. (1972). *J. Am. Chem. Soc.* **94**, 4608–4614.
Angermund, K., Claus, K. H., Goddard, R. & Krüger, C. (1985). *Angew. Chem. Int. Ed.* **24**, 237–356.
Beckmann, P. (1981). *Chem. Phys.* **63**, 359–375.
Beckmann, P. (1989). *Phys. Rev. B*, **39**, 12248–12249.
Beckmann, P. A., Al-Hallaq, H. A., Fry, A. M., Plofker, A. L. & Roe, B. A. (1994). *J. Chem. Phys.* **100**, 752–753.
Beckmann, P. A., Burbank, K. S., Clemo, K., Slonaker, E. N., Averill, K., Dybowski, C., Figueroa, J. S., Glattfelder, A., Koch, S., Liable-Sands, L. M. & Rheingold, A. L. (2000). *J. Chem. Phys.* **113**, 1958–1965.
Beckmann, P. A., Buser, C. A., Gulifer, K., Mallory, F. B., Mallory, C. W., Rossi, G. M. & Rheingold, A. L. (2003). *J. Chem. Phys.* **118**, 11129–11138.
Beckmann, P. A., Dougherty Jr, W. G. & Kassel, W. S. (2009). *Solid State Nucl. Magn. Res.* **36**, 86–91.
Beckmann, P. A., Hill, A. I., Kohler, E. B. & Yu, H. (1988). *Phys. Rev. B*, **38**, 11098–11111.
Beckmann, P. A., Paty, C., Allocco, E., Herd, M., Kurantz, C. & Rheingold, A. L. (2004). *J. Chem. Phys.* **120**, 5309–5314.
Behm, H., Lourens, A. F., Beurskens, P. T., Prinsen, W. J. C., Hajee, C. A. J. & Laarhoven, W. H. (1988). *J. Crystallogr. Spectrosc. Res.* **18**, 465–470.
Bendeif, E.-E., Lecomte, C. & Dahaoui, S. (2009). *Acta Cryst.* B**65**, 59–67.
Bruker (2007). *APEX*2 (Version 2.1-4), *SAINT* (Version 7.34A) and *SADABS* (Version 2007/4). Bruker AXS Inc., Madison, Wisconsin, USA.
Bruno, I. J., Cole, J. C., Edgington, P. R., Kessler, M., Macrae, C. F., McCabe, P., Pearson, J. & Taylor, R. (2002). *Acta Cryst.* B**58**, 389–397.
Bürgi, H. B., Capelli, S. C. & Birkedal, H. (2000). *Acta Cryst.* A**56**, 425–435.
Cowley, A. H., Decken, A., Norman, N. C., Krüger, C., Lutz, F., Jacobsen, H. & Ziegler, T. (1997). *J. Am. Chem. Soc.* **119**, 3389–3390.
Desiraju, G. R. (2002). *Acc. Chem. Res.* **35**, 565–573.
Desiraju, G. R. (2007). *CrystEngComm.* **9**, 91–92.
Dittrich, B., McKinnon, J. J. & Warren, J. E. (2008). *Acta Cryst.* B**64**, 750–759.
Ermer, O. & Neudörfl, J. (2001). *Helv. Chim. Acta*, **84**, 1268–1313.
Farrugia, L. J. (1999). *J. Appl. Cryst.* **32**, 837–838.
Frank, G. W., Hefelfinger, D. T. & Lightner, D. A. (1973). *Acta Cryst.* B**29**, 223–230.
Frey, J., Nugiel, D. A. & Rappoport, Z. (1991). *J. Org. Chem.* **56**, 466–469.
Fry, A. M., Beckmann, P., Fry, A. J., Fox, P. C. & Isenstadt, A. (1991). *J. Chem. Phys.* **95**, 4778–4782.
Gavezzotti, A. (2003). *OPiX*. University of Milano, Italy.
Gavezzotti, A. & Filippini, G. (1994). *J. Phys. Chem.* **98**, 4831–4837.
Gutsche, C. D. & Lin, L.-G. (1986). *Tetrahedron*, **42**, 1633–1640.
Handal, J., White, J. G., Franck, R. W., Yuh, Y. H. & Allinger, N. L. (1977). *J. Am. Chem. Soc.* **99**, 3345–3349.
Hark, T. E. M. van den & Noordik, J. H. (1973). *Cryst. Struct. Commun.* **2**, 643–646.
Hazell, A. C. & Lomborg, J. G. (1972). *Acta Cryst.* B**28**, 1059–1064.
Hirshfeld, F. L. (1976). *Acta Cryst.* A**32**, 239–244.
Johnson, S. A. & Hawthorne, M. F. (1991). Personal communication.
Kennedy, R. D., Ayzner, A. L., Wanger, D. D., Day, C. T., Halim, M., Khan, S. I., Tolbert, S. H., Schwartz, B. J. & Rubin, Y. (2008). *J. Am. Chem. Soc.* **130**, 17290–17292.
Khuong, T.-A. V., Dang, H., Jarowski, P. D., Maverick, E. F. & Garcia-Garibay, M. A. (2007). *J. Am. Chem. Soc.* **129**, 839–845.
Macrae, C. F., Bruno, I. J., Chisholm, J. A., Edgington, P. R., McCabe, P., Pidcock, E., Rodriguez-Monge, L., Taylor, R., van de Streek, J. & Wood, P. A. (2008). *J. Appl. Cryst.* **41**, 466–470.
Maverick, E. & Dunitz, J. D. (1987). *Mol. Phys.* **62**, 451–459.
Maverick, E. F., Knobler, C. B., Khan, S., Canary, J. W., Dicker, I. B. & Trueblood, K. N. (2003). *Helv. Chim. Acta*, **86**, 1309–1319.
Maverick, E., Mirsky, K., Knobler, C. B., Trueblood, K. N. & Barclay, L. R. C. (1991). *Acta Cryst.* B**47**, 272–280.
McMullan, R. K., Klooster, W. T. & Weber, H.-P. (2008). *Acta Cryst.* B**64**, 230–239.
Phillips, D. J. (2002). PhD Thesis. University of Nevada, Reno.
Rango, C. de, Tsoucaris, G., Declercq, J. P., Germain, G. & Putzeys, J. P. (1973). *Cryst. Struct. Commun.* **2**, 189–192.
Rheingold, A. L., DiPasquale, A. G. & Beckmann, P. A. (2008). *Chem. Phys.* **345**, 116–118.
Rosenfield, R. E., Trueblood, K. N. & Dunitz, J. D. (1978). *Acta Cryst.* A**34**, 828–829.
Sakai, T. (1978). *Acta Cryst.* B**34**, 3649–3653.
Sasaki, S., Murakami, F. & Yoshifuji, M. (1999). *Angew. Chem. Int. Ed.* **38**, 340–343.
Schomaker, V. & Trueblood, K. N. (1998). *Acta Cryst.* B**54**, 507–514.
Seeman, J. I., Secor, H. V., Breen, P. J., Grassian, V. H. & Bernstein, E. R. (1989). *J. Am. Chem. Soc.* **111**, 3140–3150.
Sheldrick, G. M. (2008). *Acta Cryst.* A**64**, 112–122.
Spek, A. L. (2003). *J. Appl. Cryst.* **36**, 7–13.
UCLA Crystallographic Package (1984). University of California, Los Angeles, USA.
Yamamoto, G. & Ōki, M. (1986). *Tetrahedron Lett.* **27**, 49–50.
Yoshifuji, M., Shima, I. & Inamoto, N. (1981). *J. Am. Chem. Soc.* **103**, 4587–4589.
Zeller, M., Lutz Jr, M. R. & Becker, D. P. (2009). *Acta Cryst.* B**65**, 223–229.